

Doctoral Thesis

Escape to Space or Return to Venus: Ion Flows Measured by Venus Express

Moa Persson

Main supervisor:

Dr. Yoshifumi Futaana

Assistant supervisors:

Dr. Hans Nilsson

Dr. Maria Hamrin

Opponent:

Dr. Dmitrij Titov

Examination committee:

Dr. Uwe Raffalski

Dr. Maria Sundin

Dr. Mikael Granvik



UMEÅ
UNIVERSITY



November 2020

Moa Persson: *Escape to Space or Return to Venus:
Ion Flows Measured by Venus Express*
© November 2020

University Department:
Faculty of Science and Technology,
Department of Physics
Umeå University, Umeå, Sweden

Ph.D. Institute:
Swedish Institute of Space Physics
Kiruna, Sweden

ISBN: 978-91-7855-378-5 (print)
ISBN: 978-91-7855-379-2 (pdf)
ISSN: 0284-1703
IRF Scientific Report 311

Printed by CityPrint i Norr AB
Umeå, Sweden 2020

Abstract

The present-day Venusian atmosphere is crushingly dense, extremely hot and arid. Yet, in its early history, Venus presumably had a massive amount of water, which, if spread evenly over the surface, provided a water depth of 10s to 100s of meters. Therefore, over the course of the atmospheric evolution, the water must have been removed from Venus. The main processes responsible for water loss can be catagorised into either diffusion into the surface materials or escape to space, where the focus of this thesis is the latter. Determining the contribution on the atmospheric evolution from each of these processes can help us understand how planetary atmospheres evolve, both here in our Solar System and in extra-solar systems, and tell us why Venus became so dry.

The water escape to space is determined by several processes, where the main processes are a consequence of the interaction between the Venusian atmosphere and the solar wind. As Venus does not have an intrinsic magnetic field, its atmosphere interacts directly with the solar wind, and creates a, so called, induced magnetosphere. The interaction causes part of the solar wind energy and momentum to be transferred to the upper atmospheric particles. The additional momentum may allow the ions to reach above escape energy and escape the planet. Therefore, the interaction between the atmosphere and the solar wind is important to study to determine the rate of escape of atmospheric constituents to space.

In this thesis, the escape of atmospheric constituents to space is investigated through measurements of the H^+ and O^+ ion flows. These ion flows were measured by the Ion Mass Analyser (IMA) on board the Venus Express spacecraft, which orbited Venus during 2006-2014. Using IMA measurements near the North Pole ionosphere, the ionospheric ion flows were shown to have a strong dusk-to-dawn component along the terminator, inside the collisional region of the atmosphere. From ion flow measurements in the magnetotail, the rate of escape of atmospheric H^+ and O^+ ions were shown to be affected by the solar cycle, with an average escape rate ratio near two, the stoichiometric ratio of water. The change is mainly attributed to the decrease in the net escape rates of H^+ , which is a result of the increase in return flows, i.e. ions that flow back towards Venus in the magnetotail. Furthermore, the O^+ net escape rate increases as the amount of energy available in the upstream solar wind increases. The increase indicates, as expected, that a portion of the available energy in the upstream solar wind is transferred to the escaping ions. However, the total portion of energy transferred from the solar wind to the escaping ions decreases as the available upstream energy increases. Using the simple relation between the O^+ escape rate and the upstream solar wind energy flux, the total atmospheric escape was extrapolated backwards in time, by accounting for the evolution of the solar wind parameters. The resulting total escape over the past 3.9 Ga can be translated into a global equivalent water depth of 0.02-0.6 m. This result cannot explain the massive historical water content on Venus.

Sammanfattning

Venus atmosfär är idag tjock, het och extremt torr, men den har inte alltid varit sån. I dess tidigare historia fanns det troligtvis mycket vatten på Venus yta. Om man skulle tagit allt det vattnet och spridit den jämnt över hela Venus yta tror man att det skulle bli ett djup på nånstans mellan 10 meter till över 100 meter. Det betyder att en stor mängd vatten har försvunnit under Venus atmosfäriska historia. Det finns i huvudsak två processer som är kapabla till att ta bort vatten från Venus: antingen reagerar vattnet med ytan och sparas inuti Venus skorpa eller kärna, eller så flyr den ut till rymden. I den här avhandlingen har fokuset legat på den senare av de två processerna. Genom att undersöka vilken av dessa processer som har haft störst inverkan på Venus atmosfäriska evolution och dess förlust av vatten kan vi förstå hur olika planeters atmosfärer utvecklas, både här i vårt eget solsystem och i extrasolära system, och specifikt hjälpa oss förstå varför Venus blivit så torr.

Flykt av vatten till rymden påverkas av flera olika processer, varav de med störst inverkan är en konsekvens av interaktionen mellan Venus atmosfär och solvinden. Eftersom Venus inte har något eget inre magnetfält interagerar atmosfären direkt med solvinden och skapar en, vad man kallar, inducerad magnetosfär. Interaktionen gör så att en del av energin och rörelsemängden i solvinden överförs till partiklarna i Venus övre atmosfär. Den extra rörelsemängden gör så att jonerna i Venus övre atmosfär kan nå över flykthastigheten på ca 10 km/s och därmed flyr från planeten. Därför är interaktionen mellan atmosfären och solvinden viktig att studera, för att förstå hur mycket partiklar som flyr från Venus.

I den här avhandlingen har flykten av atmosfäriska partiklar till rymden undersökts med hjälp av mätningar av flöden av vätejoner (H^+) och syrejoner (O^+). Dessa jonflöden har mätts av instrumentet Ion Mass Analyser (IMA), en del av ASPERA-4, ombord på satelliten Venus Express. Venus Express fanns i omloppsbana runt Venus under 2006-2014 och gav mätningar under dess mer än 3000 varv runt Venus. Dessa mätningar har i den här avhandlingen använts för att räkna ut medelvärden av jonflödena i både jonosfären (övre delen av atmosfären) och magnetosvansen (den långa förlängningen av den inducerade magnetosfären på nattsidan av Venus), för att undersöka solvindens inverkan på Venus atmosfäriska evolution.

Jonflöden mätta av IMA nära Venus nordpol visar att flödet inte endast rör sig från dag till natt, som tidigare hittats vid ekvatorn av den tidigare missionen Pioneer Venus. Istället har flödet en komponent längs med terminatorn, eller dag-natt linjen, från kväll mot morgon. Detta flöde finns ända ner på höjder där kollisioner är viktiga. Jonflöden mätta av IMA i Venus magnetosvans visar att flykten av H^+ och O^+ joner från atmosfären ändras över solcykeln, och att förhållandet mellan deras flykt ligger nära två, som indikerar att det kommer från vatten (två väteatomer och en syreatom). Ändringen i förhållandet kommer främst från att flyktflödet för H^+ minskade, vilket till största delen beror på en ökning av returflöden, alltså joner som flödar tillbaka mot Venus i

magnetosvansen. Dessutom ökade flykten av O^+ när mängden energi tillgänglig i solvinden ökade. Denna ökning indikerar, som förväntat, att energi överförs från solvinden till jonerna, vilket leder till att jonerna kan fly från Venus. Dock minskade andelen energi som överfördes till jonerna när energin i solvinden uppströms ökade. Genom att använda en enkel relation mellan flykten av O^+ och energiflödet i solvinden, och genom att ta hänsyn till evolutionen av solvinden, kan flykten extrapoleras bakåt i tiden. På så sätt kan man ta reda på hur mycket som totalt har flytt i form av joner från Venus under de senaste 3.9 miljarder åren. Den totala mängd som flytt kan översättas till ett vattendjup på 0.02-0.6 meter, om man antar att allt syre kommer från vatten och sprider vattnet jämnt över hela Venus yta. Den totala mängd vatten som flytt från Venus som joner, som beräknats här, kan inte beskriva hur den massiva mängd vatten på tiotals till hundratals meter, som man tror existerade på Venus i dess tidigare historia, försvunnit. Det betyder att Venus antingen inte hade så mycket vatten i dess tidigare historia som man tidigare trott, eller att den största mängden vatten istället försvunnit genom andra processer.

List of appended papers

Paper I

M. Persson, Y. Futaana, A. Fedorov, H. Nilsson, M. Hamrin, and S. Barabash (2018), “H⁺/O⁺ escape rate ratio in the Venus magnetotail and its dependence on the solar cycle”. *Geophysical Research Letters*, doi: 10.1029/2018GL079454

Paper II

M. Persson, Y. Futaana, H. Nilsson, G. Stenberg Wieser, M. Hamrin, A. Fedorov, T. Zhang, and S. Barabash (2019), “Heavy ions in the upper ionosphere of the Venusian North Pole”. *Journal of Geophysical Research: Space Physics*, doi: 10.1029/2018JA026271

Paper III

M. Persson, Y. Futaana, R. Ramstad, K. Masunaga, H. Nilsson, M. Hamrin, A. Fedorov, and S. Barabash (2020a). The Venusian atmospheric oxygen ion escape: Extrapolation to the early Solar System. *Journal of Geophysical Research: Planets*. Doi: 10.1029/2019JE006336

Paper IV

M. Persson, Y. Futaana, R. Ramstad, A. Schillings, K. Masunaga, H. Nilsson, A. Fedorov, and S. Barabash (2020b). Global Venus-solar wind coupling and oxygen ion escape. Submitted for publication in *Geophysical Research Letters*.

Paper V

M. Persson, Y. Futaana, A. Fedorov, and S. Barabash (2020c). Return flows in the Venusian magnetotail measured by Venus Express. To be submitted for publication in *Journal of Geophysical Research: Space Physics*.

List of related papers

K. Masunaga, Y. Futaana, **M. Persson**, S. Barabash, T. Zhang, Z. Rong, and A. Fedorov. “Effects of the solar wind and the solar EUV flux on O⁺ escape rates from Venus”. *Icarus*. Doi: 10.1016/j.icarus.2018.11.017

A. Bader, G. Stenberg Wieser, M. Andre, M. Wieser, Y. Futaana, **M. Persson**, H. Nilsson, and T. L. Zhang (2019) “Proton temperature anisotropies in the plasma environment of Venus”. *Journal of Geophysical Research: Space Physics*. Doi: 10.1029/2019JA026619

G. Collinson, D. Sibeck, N. Omid, J. Grebowsky, J. Halekas, D. Mitchell, J. Espley, T. Zhang, **M. Persson**, Y. Futaana, and B. Jakosky (2017) “Spontaneous hot flow anomalies at Mars and Venus”. *Journal of Geophysical Research: Space Physics*. Doi:10.1002/2017JA024196

S. S. Limaye, S. Lebonnois, A. Mahieux, M. Pätzold, S. Bougher, S. Bruinsma, S. Chamberlain, R. T. Clancy, J.-C. Gerard, G. Gilli, D. Grassi, R. Haus, M. Herrmann, T. Imamura, E. Kohler, P. Krause, A. Migliorini, F. Montmessin, C. Pere, **M. Persson**, A. Piccialli, M. Rengel, A. Rodin, B. Sandor, M. Sornig, H. Svedhem, S. Tellmann, P. Tanga, A. C. Vandaele, T. Widemann, C. F. Wilson, I. Müller-Wodarg, and L. Zasova (2017) “The Thermal Structure of the Venus Atmosphere: Intercomparison of Venus Express and Ground Based Observations of Vertical Temperature and Density Profiles”, *Icarus*, doi: 10.1016/j.icarus.2017.04.020

Acknowledgments

First of all I would like to give many thanks to my main supervisor Yoshifumi Futaana. We've had many fun discussions on science, how to write more beautiful code, and how to become a good scientist. This thesis would not have been realised without your constant support. Thank you also to my co-supervisors Hans Nilsson, for the many interesting discussions and ideas and for taking the time when I struggled, and Maria Hamrin, for our many discussions on "meta-physics" that have made me evolve as a scientist in more than just my knowledge of physics. I also want to thank SNSA for providing the funding for my PhD studies (Dnr: 129/14), and to Mats and Futaana for the additional year with archiving work.

I would like to give my sincerest thanks to Stas Barabash and everyone else in my research group Solar System Physics and Technology (SSPT). Many long meetings have led to many new insights.

I am so happy to have met and worked with the many young people, like me, that I have encountered at IRF and all over the world: Robin, Kei, Laura, Charles, Hans, Jesper, Pegah, Joan, Richard, George, Diana, Maike, Rikard, Angèle, Philipp, Daniel, Hayley, Sebastián, Anja, Shaosui, and many more. I am especially happy to have met the trio Etienne, Máté, and Audrey. IRF would have been much less fun without your constant source of laughter, mischief and wild discussions. Specifically, I would like to thank Audrey for the many long discussions in your office; starting a PhD at the same time makes a great friend for life. Of course, I cannot forget to thank everyone for the many hours of lunch-Pingis that not only made me a better player, but increased my happiness level overall. Thank you all for making my PhD time so awesome.

I am so happy to have spent these years at IRF, where everyone feels like part of a family, and the parties are never boring. Thank you all for being so friendly and supportive. Thank you to Rick for providing so many English proof readings.

I want to thank everyone else I have met during my so far short, but hopefully becoming very long, career within science and research. To Janet Luhmann and Dave Mitchell for hosting me for a few months at SSL, UC Berkeley. I learnt so much in such a short time. To Andrei Fedorov for our many discussions on the workings on the instrument, and your invaluable work on the calibration. A scientist's most important tools are truly "experience and imagination".

To Sofia, for the unconditional support and encouragements when I struggle, for sharing the many moments of happiness, and for the love. Without you life would be so so boring.

To my family for the love and the never-ending support of my interest in learning and my ambitions throughout my life. Without you I wouldn't be here.

To myself, for finishing this thesis amidst a large horrible COVID-19 virus pandemic situation, which moved my defense to a later date, but also gave me more time to finish my thesis and additional papers: "I am big enough to admit that I am often inspired by myself" (Leslie Knope, Parks and Recreation).

Credits

The L^AT_EX template used in this thesis is developed by Mathias Legrand and is licensed under CC BY-NC-SA 3.0 license numbers. The credits for the chapter headings used in the thesis are as follows: The Contents and chapter 5 head figures of Venus is an image processed from 78 Mariner 10 frames captured through orange and ultraviolet filters. It is intended to look approximately natural in color, though the use of the ultraviolet images makes cloud patterns more visible than they would be to the human eye, credit: NASA/JPL/Mathias Malmer. The chapter 1 head figure is a copy of the painting "The birth of Venus" by Sandro Botticelli. The chapter 2 head figure is a copy of the painting "Starry night" by Vincent van Gogh. The chapter 3 head figure is an artist's impression of the interaction between Venus and the solar wind, credits: ESA/C. Carreau. The chapter 4 head figure is an artist's view of ESA's Venus Express probe in orbit around Venus, credit: ESA/D. Ducros. The chapter 6 head figure is an image of Venus taken by JAXA's Akatsuki spacecraft, which have been processed by Damia Bouic, credit: JAXA/ISAS/DARTS/Damia Bouic. The chapter 7 head figure is a combination of images of Venus, Earth and Mars made by ESA. The bibliography head figure is a composite of radar measurements of the Venusian surface gained by the Magellan and Pioneer Venus spacecraft, credit: NASA/JPL-Caltech.



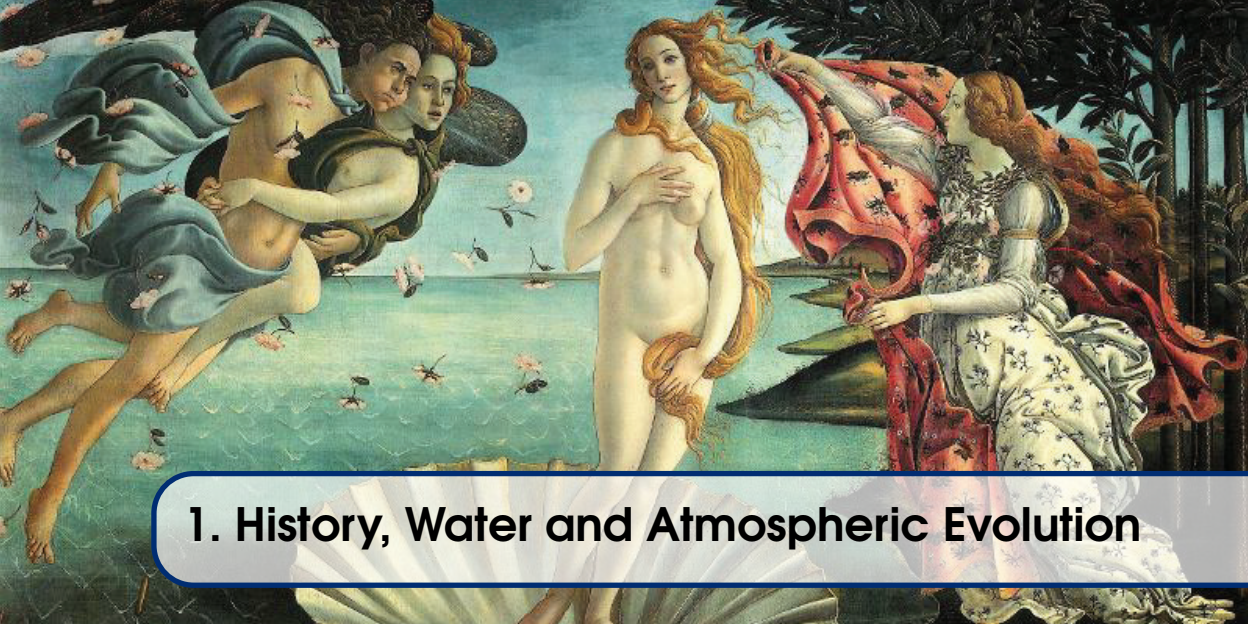
Contents

	Abstract	iii
	Sammanfattning	v
	List of appended papers	vii
	List of related papers	ix
	Acknowledgements	xi
	Credits	xiii
1	History, Water and Atmospheric Evolution	1
2	Plasma Environment Near Venus	7
2.1	Atmosphere and Ionosphere of Venus	7
2.2	Solar Wind near Venus orbit	10
2.3	The Venusian Induced Magnetosphere	11
3	Atmospheric Escape	15
3.1	Thermal Escape	16
3.1.1	Jeans' Escape	16

3.1.2	Hydrodynamic Escape	16
3.2	Non-thermal Escape	17
3.2.1	Photochemical Reactions	17
3.2.2	Pickup ions	18
3.2.3	Atmospheric Sputtering	19
3.2.4	Magnetotail escape - Momentum transfer, Cold Plasma Outflow and Plasma Instabilities	20
3.3	Summary of Measured Escape Rates at Venus	21
4	Instrumentation and Methods	25
4.1	Venus Express	25
4.2	MAG	25
4.3	ASPERA-4/IMA	26
4.3.1	Energy Table Corrections for Low Altitude Measurements . . .	28
4.3.2	Mass Separation of Heavy Ions	30
4.3.3	Separation of Solar Wind and Planetary Protons in the Magneto- tail	31
4.4	Calculating Ion Properties from an Ion Spectrometer	33
4.4.1	Correcting Measurements for the Spacecraft Velocity	34
4.4.2	Calculating Average Escape Rates	34
4.4.3	Calculating the Standard Error on the Escape Rates	36
5	Ion Flows near the North Pole Ionosphere . . .	39
5.1	General Flow Patterns	39
5.2	Altitude Profiles	40
5.3	Coupling with Neutrals and Effect on Escape Rates	41
6	Ion Escape Through the Magnetotail	43
6.1	H⁺ and O⁺ Ion Escape Over the Solar Cycle	43
6.2	Return Flows in the Magnetotail	43
6.3	O⁺ Ion Escape Dependence on Upstream Parameters	47
6.4	Coupling Between Solar Wind and Escaping Ions	47
6.5	Extrapolating the Escape Rates to 3.9 Ga	48
7	Conclusions and Implications	51
7.1	Venus, Earth and Mars	52
7.2	Water on Venus	53
7.3	Life on Venus	54
7.3.1	Past	54

7.3.2	Present	54
7.3.3	The future is ♀?	55
7.4	Desired New Measurements in the Future	56
7.4.1	Space Weather Events	56
7.4.2	Ionosphere-Thermosphere Coupling	57
7.4.3	Sputtering	58
7.4.4	Ongoing Mission Concepts	59

Bibliography	63
-------------------------------	-----------



1. History, Water and Atmospheric Evolution

“The universe is hilarious! Like, Venus is 900 degrees¹. I could tell you it melts lead. But that’s not as fun as saying, “You can cook a pizza on the windowsill in nine seconds.” And next time my fans eat pizza, they’re thinking of Venus!”

– Niel DeGrasse Tyson

The planet Venus is one of the brightest objects on the night sky, but is only visible during either morning or evening, as it orbits the Sun at a closer distance than Earth. Due to its brightness, Venus appears as a bright morning or evening star, and has been observed by humans through many early civilisations. The planet therefore acquired many different names, often related to the Gods and Goddesses of the early civilisations. These deities were often related to brightness or beauty. For example, the Greeks named the morning star Lucifer (“light-bringer” in latin) and the evening star Vesper (“evening” in latin), which both were sons of Aurora, the Goddess of dawn. The Greeks realised that the morning and evening stars were the same object at around 300 B.C., but even so the dual names prevailed long after. The Romans believed that the planet, which the Greeks had named Lucifer, was connected to Venus, the Goddess of love and beauty, which was married to Mars, the God of war. The Roman name of the planet is still used in the scientific community today. The famous painting “the birth of Venus”, by Sandro Botticelli, from the history of the Goddess Venus in Roman mythology, is shown in the chapter heading above.

In the earlier human history the ancient Sumarians of Mesopotamia named the planet after Innana, or Ishtar, the Goddess of both love and war. In India, the planet was named Shukra (“brightness” in sanskrit), after the powerful saint

¹900°F ≈ 480°C

Shukra. While, in Norse mythology, the planet was named after Frigg (“Frig-gjarstjarnan”), the Goddess of marriage, the most powerful of all Goddesses, which was married to Odin, the God of war and wisdom. As evident, Venus has long been awed by humans and still appears often in culture. In “the starry night” by Vincent van Gogh, Venus appears as one of the brightest stars in the painting (see chapter 2 head figure), which was realised after calculations showed that Venus should have appeared through the window of van Gogh’s room around the time the painting was made.

After the invention of the telescope it was realised that the planet Venus is covered with thick clouds, and that the surface cannot be seen in visible light. It was hypothesised that Venus might be covered with life (e.g. Morowitz and Sagan, 1967), which cannot be seen through the thick cloud cover, and with the curiosity an interest grew on exploring the planet beneath its thick cloud cover.

With the development of spacecraft in space, starting with Sputnik in 1957, humans started to send spacecraft to Venus. The first flyby was made in 1962 by NASA’s Mariner 2 mission (see Figure 1.1), which was later accompanied by Mariner 5 and 10 in 1967 and 1974, respectively. The Mariner missions showed that Venus does not have a strong intrinsic magnetic field, in contrast with Earth (see Table 1.1), and that the Venusian atmosphere interacts directly with the solar wind, a fast stream of plasma ejected from the Sun. The interaction forms a, so called, induced magnetosphere around Venus (Bridge et al., 1976; Gringauz et al., 1968). In the meantime, the Soviet Venera mission series was initiated. The first successful probe to delve into the atmosphere was Venera 4 in 1967, but it was crushed by the thick atmosphere before it could reach the surface. The probe measured the density, temperature and pressure structures and showed that the atmosphere is composed of $>90\%$ CO_2 (Vinogradov et al., 1968). Soviet continued to send probes to Venus, and finally Venera 7 was the first successful mission to reach the surface (see review by Marov, 1972). Although it was more a violent crash than a landing, the Venera 7 probe provided an improved knowledge of the hellish conditions at the lower part of the Venusian atmosphere, where the temperature is more than 460°C and the air pressure is 92 times that at the surface of Earth. These findings made it clear that life, as we know it on Earth, could not exist on Venus. In 1975, the Venera 9 and 10 missions included landers that managed to take the first pictures of the surface, and the first orbiters around Venus. Finally, in 1984 Venera 15 and 16 concluded the Venera mission series after orbiting Venus for several months. During its time, the Venera missions gave us the first initial understanding of the atmosphere and its interaction with the solar wind (see review by Breus, 1979). A summary of the most important characteristics of Venus and its atmosphere are provided in Table 1.1, together with a comparison with Earth.

The two main missions that made plasma measurements was the Pioneer Venus Orbiter (PVO; Colin, 1980) and Venus Express (VEx; Svedhem et al., 2007). PVO orbited Venus during 1978-1992, and provided the basic understanding of the Venusian interaction with the solar wind. It included

several plasma instruments for ions and electrons. VEx orbited Venus during 2006-2014, and further extended the picture of the Venus solar wind interaction, and the escape rates' potential effect on the atmospheric evolution (see review by Futaana et al., 2017). Figure 1.1 shows a summary of all the past, and future planned, plasma instruments included on board the different missions near Venus. The instrument energy ranges are indicated, as well as the average ranges of ion and electron energy for each of the regions in the Venusian plasma environment (chapter 2). Magnetic field measurements are not included in Figure 1.1, but is a very important addition to plasma measurements, and was conducted by many missions, including PVO and VEx.

One of the most important open questions still remaining is why the Venusian atmosphere is so different from Earth's atmosphere today. Specifically, Venus has an extremely hot and arid atmosphere today, but there are several studies pointing towards that Venus had a significant amount of water in its early history (e.g. Donahue et al., 1997; Donahue and Hartle, 1992; Grinspoon, 1993; Taylor and Grinspoon, 2009). If spread equally over the Venusian surface the water would presumably have reached water depths of 10s to 100s of meters (Way et al., 2016). An important question is therefore how the water disappeared from the Venusian atmosphere. To understand this evolution, the issue need to be addressed from several directions. Questions on how the initial atmosphere was composed, how the interaction between the surface and the atmosphere acted throughout the Venusian history, and in what way the escape of atmospheric particles to space has influenced the evolution of the atmosphere need to be answered. Determining how large contribution each part had on the atmospheric evolution in the past and in the present will provide the key insights into why the water disappeared from Venus. In addition, the results will be important for understanding the atmospheric evolution of planets in our Solar System and extra-solar systems alike. In this thesis, this question is addressed from the point of view on the interaction between the atmosphere and space, i.e. how the plasma environment of Venus has affected the evolution of the Venusian atmosphere through the escape of atmospheric constituents to space.

In the next chapter a summary of the Venusian plasma environment is provided, and in chapter 3 the most important escape channels are discussed. As measurements made by VEx was used in this thesis, detailed information on VEx is provided in chapter 4. chapter 5 and chapter 6 discusses the results of this thesis work and chapter 7 concludes the thesis and discusses the implications of the results on the evolution of the Venusian atmosphere.

Table 1.1: Basic characteristics of Venus.

	Venus	Earth
Mass	$4.87 \cdot 10^{24}$ kg	$5.97 \cdot 10^{24}$ kg
Radius, R_V	6052 km	6371 km (average)
Ellipticity	0.000	0.003
Mass of atmosphere	$4.8 \cdot 10^{20}$ kg	$5.15 \cdot 10^{18}$ kg
Major atmospheric constituents	96.5 % CO ₂ , 3.5 % N ₂	78 % N ₂ , 21 % O ₂ , 1 % Ar
Surface temperature	462°C (735 K)	15°C (287 K)
Surface pressure	92 bar	1 bar
Bond albedo	0.77	0.29
Distance from Sun	0.73 AU (108 209 475 km)	1 AU (149 597 871 km)
Mean orbital speed	35 km/s	29.8 km/s
Eccentricity	0.0067	0.0167
Orbit inclination	3.39°	7.16°
Planet inclination	177.4°	23.4°
Length of year	224.7 Earth days	365.2 Earth days
Rotation period	5832 h (243 d)	23.9 h (1 d)
Length of day	2802 h (117 d)	24 h (1 d)
Moons	None	1 (The Moon)
Magnetic moment	$< 8.4 \cdot 10^{10}$ T m ³	$7.8 \cdot 10^{15}$ T m ³
Escape velocity at surface (v_{esc})	10.36 km/s	11.19 km/s

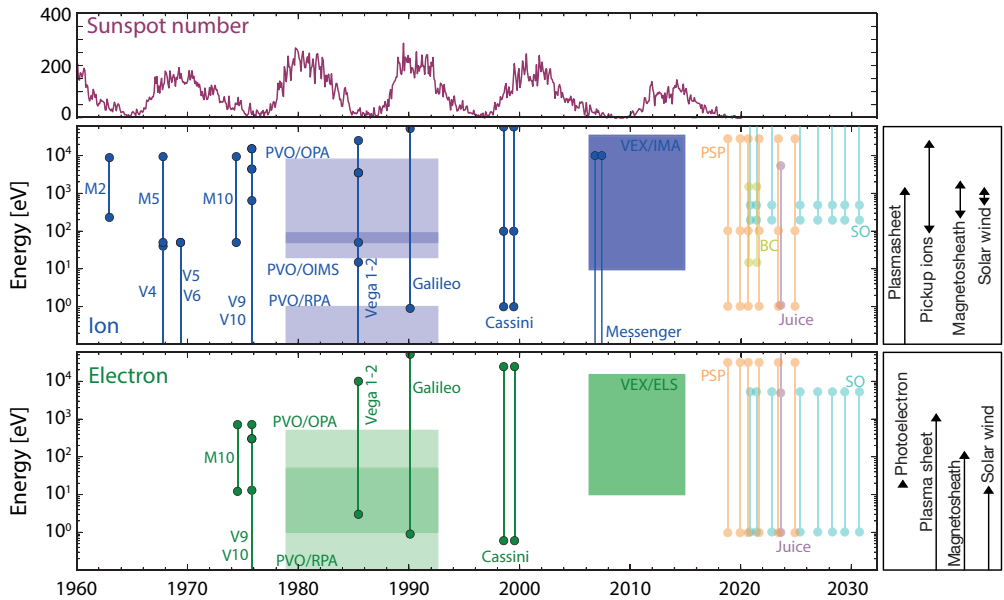
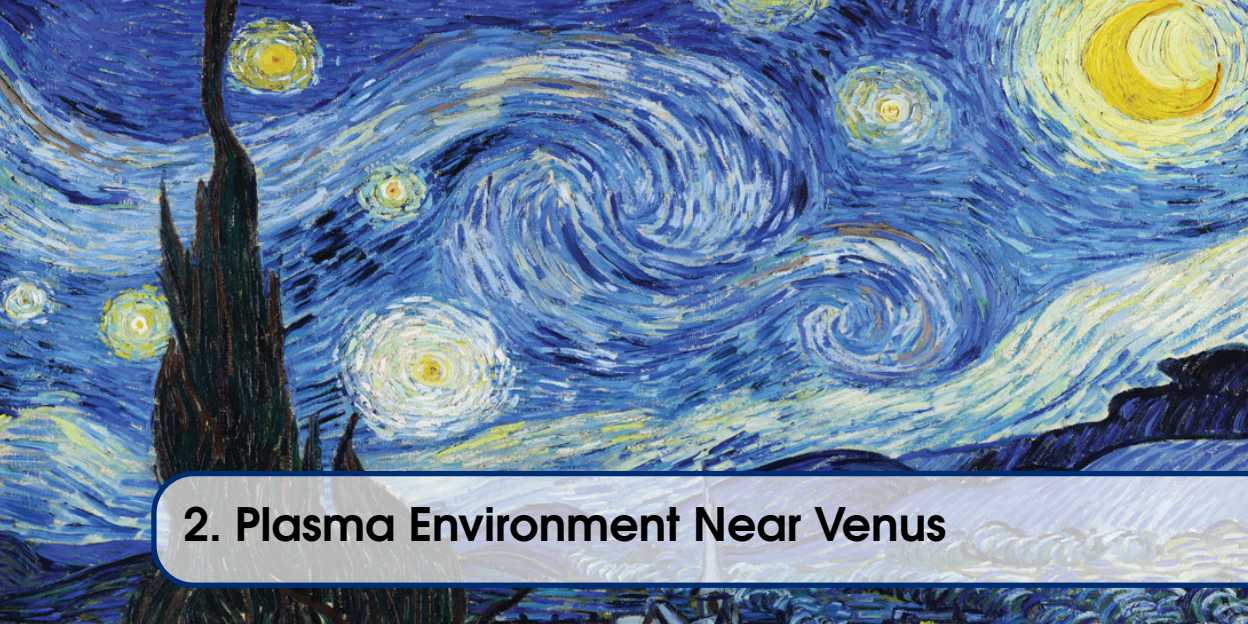


Figure 1.1: Summary of plasma experiments that made measurements in the near-Venus space. Included is also the sunspot numbers, which indicates the solar cycle, and the range of energy for ions and electrons, respectively, in each plasma domain around Venus. Several future flybys are also included (see more details in subsection 7.4.4) (Adapted from Futaana et al., 2017).



2. Plasma Environment Near Venus

2.1 Atmosphere and Ionosphere of Venus

The atmosphere of Venus is crushingly thick, with a total mass 92 times that of Earth's atmosphere. It is mainly composed of carbon dioxide (96.5 %, CO_2), with a smaller content of nitrogen (3.5 %, N_2) and other species (< 1 %) (see Table 1.1). The CO_2 acts as a greenhouse gas that causes the lower atmosphere of Venus to have a temperature of above 460°C . However, in the upper atmosphere the CO_2 acts in an opposite manner. Here, it emits radiation at $13.7\text{ }\mu\text{m}$, effectively cooling the upper atmosphere. The cooling means that the upper atmosphere is not extended to very high altitudes. The exobase, the altitude above which collisions between particles are no longer important, is located at around 200 km on Venus, while for Earth, which is mostly composed of N_2 and does not have a significant CO_2 cooling, the exobase is located at above 500 km. This is important for the interaction between the solar wind and Venus, which is further discussed in section 2.3.

An outstanding characteristic of the Venusian atmosphere is the winds. The lower atmosphere has a retrograde superrotation, with winds increasing from a few m/s at the surface to several 100s m/s above 60 km altitude (Schubert et al., 1980). The cloud layer, located at around 60 km, is therefore moving around the planet in only around 4 days, which can be compared to the 243 days it takes for the solid planet itself. The wind speeds are decreasing from the equator towards the pole, which give the clouds its characteristic V-shape (Schubert et al., 1980). The superrotation is a consequence of angular momentum being redistributed in the atmosphere by tides and planetary scale waves (e.g. Horinouchi et al., 2020; Read and Lebonnois, 2018). On the other hand, in the upper atmosphere the winds are driven by the heating on the dayside from the solar radiation. Due to the long days and nights, the atmosphere is heated and expanded on the

dayside, creating a pressure gradient along the day-night line. The pressure gradient creates a force on the atmospheric particles, and a subsolar-to-antisolar (SS-AS) flow is formed. The SS-AS flow is dominating above 100 km altitude, which means that between 60-100 km there is a transition region between the superrotating flow and the SS-AS flow (Keating et al., 1985).

The upper atmosphere on the dayside is exposed to the incoming extreme ultraviolet (EUV) radiation from the Sun. The EUV radiation ionises part of the exposed particles. The ionisation starts a chain of chemical reactions in the upper atmosphere



The reactions cause the upper atmosphere (above ~ 150 km) to be dominated by O, and not CO_2 . Figure 2.1a show the modelled neutral densities based on data from the neutral mass spectrometer on board PVO (solid lines; Hedin et al., 1983; Niemann et al., 1980), with the minor species from Fox and Sung (2001) thermosphere-ionosphere model (dashed lines). The chemical reactions in Equation 2.1 are also responsible for the maintenance of the ionosphere, which is mainly composed of O^+ and O_2^+ ions (Fox and Sung, 2001). Figure 2.1b show the density of the main ion species in the upper ionosphere measured by the ion spectrometer on board PVO (Taylor et al., 1980).

As the ionosphere is mainly maintained by the ionisation from solar EUV radiation of ions on the dayside, it was a big surprise to find that Venus has an extensive nightside ionosphere. The slow rotation of Venus, combined with the short ion lifetime and the low ionisation rate due to electron impacts, should not allow for a high nightside ion density (Butler and Chamberlain, 1976). The discrepancy is explained by considering that the ions in the upper ionosphere are transported to the nightside ionosphere by winds. Consistently, PVO observed ions flowing with speeds of 2-5 km/s from dayside to nightside near the terminator (Knudsen et al., 1980).

To explain this day-to-night flow we need to take into account which forces act to accelerated the ions. Ions are accelerated by electric fields, which can be described by the generalised Ohm's law

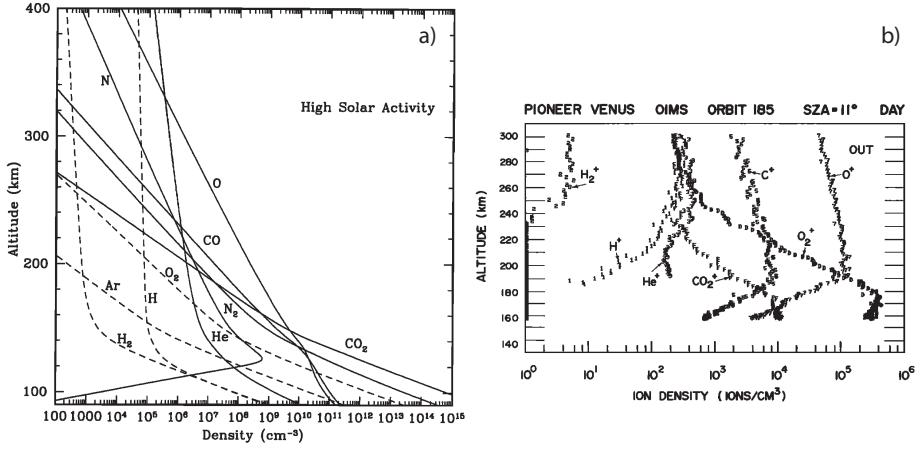


Figure 2.1: a) Modelled neutral densities using fitted spherical harmonics to the measurements by ONMS onboard PVO (solid lines; Hedin et al., 1983), which was extended to minor species (dashed lines) by the self-consistent model of Fox and Sung (2001). b) Ion densities measured near the subsolar point, during one orbit, by the OIMS instrument onboard PVO (Taylor et al., 1980)

$$\vec{E} = \underbrace{-\vec{v}_i \times \vec{B}}_{\vec{E}_{conv}} + \underbrace{\frac{1}{qn_e} \vec{j} \times \vec{B}}_{\vec{E}_{Hall}} - \underbrace{\frac{1}{qn_e} \nabla P_e}_{\vec{E}_{ambi}}, \quad (2.2)$$

where \vec{v}_i is the bulk velocity of the ions, \vec{j} is the current density, n_e is the electron density, q is the ion charge, and ∇P_e is the electron pressure gradient (see e.g. Dubinin et al., 2011). The three components of the electric field describe the effect from the motion of the ion in a magnetic field (convective electric field, \vec{E}_{conv}), from currents perpendicular to the magnetic field (Hall term, \vec{E}_{Hall}) and from electron pressure gradients (ambipolar electric field, \vec{E}_{ambi}).

Knudsen et al. (1981) suggested that the day-to-night flow in the ionosphere is driven by a thermal pressure gradient (\vec{E}_{ambi} , the 3rd term in Equation 2.2), namely the large pressure gradient ∇P_e between the night- and dayside caused by the heating and ionisation on the dayside. An order of magnitude calculation show that the pressure gradient would provide a stronger force on the ions than the magnetic pressure (\vec{E}_{Hall} , the 2nd term in Equation 2.2) (Knudsen et al., 1981). On the other hand, Perez-de-Tejada (1986) and Lundin et al. (2014) suggest that a momentum transfer from the solar wind plasma flow to the cold Venusian ionospheric plasma can explain the day-to-night flows in the upper ionosphere. The momentum transfer is found through using two differential streaming species, solar wind protons p and planetary O^+ o , with an average

bulk velocity

$$\vec{v}_i = \frac{n_p q_p}{n_p q_p + n_o q_o} \vec{v}_p + \frac{n_o q_o}{n_p q_p + n_o q_o} \vec{v}_o \quad (2.3)$$

and including it in the momentum equation, which for the O^+ ion is thus, assuming that $n_e = n_o + n_p$ and $q_p = q_o = e$, (Dubinin et al., 2011)

$$m_o n_o \frac{d\vec{v}_o}{dt} = \frac{e n_p n_o}{n_e} (\vec{v}_o - \vec{v}_p) \times \vec{B} + \frac{n_o}{\mu_0 n_e} \vec{j} \times \vec{B} + \frac{n_o}{n_e} \nabla P_e, \quad (2.4)$$

where the first term describe the momentum gain of the planetary O^+ ions from the solar wind protons.

Which force is the major force acting on the ions depends on the characteristics of the ionosphere and, thus, is likely a function of altitude. At the lower altitudes the ions are more dependent on pressure gradients, while at higher altitudes, near the boundary between the ionosphere and the solar wind flow, collisions are less important and the momentum transfer from the solar wind becomes more important.

With a flow of 2-5 km/s, a significant amount of ions is provided to the nightside. Assuming that the same flow accounts for the entire disk, a total of $5 \cdot 10^{26}$ ions/s flow from day-to-night (Knudsen and Miller, 1992). The flow can supply the nightside ionosphere, where the ions eventually can escape to space. Escape processes are further discussed in chapter 3.

2.2 Solar Wind near Venus orbit

The solar wind is a stream of ionised plasma, expanding supersonically outward from the solar corona and into interplanetary space. The average velocity of the solar wind in the interplanetary space is 400 km/s, but it can range from 100 km/s to over 1000 km/s for some extreme events. It is mainly composed of protons and electrons, with a few percent of alpha particles. A small component ($<1\%$) of heavier elements is also included. As the solar wind propagates through the interplanetary space, its density decreases with one over the square of the distance. The density in the near-Venusian space is usually 10 particles cm^{-3} but also ranges depending on the solar wind transient events.

Due to the strong magnetic fields in the solar corona, originating from the solar interior, the expanding solar wind plasma is highly magnetised, frequently referred to as a “frozen in” condition (Alfvén, 1957). As the solar wind propagates outward, the solar wind plasma pulls the magnetic field with it and forms the so called Interplanetary Magnetic Field (IMF). The combination of the expanding solar wind and the rotation of the Sun leads to a spiral structure of the IMF, the Parker spiral (Parker, 1958). As the solar wind plasma moves outward throughout the Solar System, the Parker spiral is stretched out, and

the angle between the radial direction from the Sun and the IMF gets larger with an increased distance from the Sun. Near Venus the Parker spiral angle is on average $\sim 40^\circ$. The average magnetic field strength is ~ 12 nT (Luhmann, 1986).

There are variations in the solar wind, both in the particle fluxes and the magnetic field. The ejection of plasma from the Sun depends on the characteristics of the solar corona. For example, at the coronal holes, the solar surface is cooler, and the solar wind is emitted at a larger speed than from the surrounding surface. As the solar wind propagates outward through the solar system, the difference in speed between different parts of the solar wind causes solar wind stream interaction regions (IRs), where the faster streams catch up to the slower streams. As the coronal holes can persist for several months, these IRs can be seen periodically from an observer in space, and are therefore denoted co-rotating IRs (CIRs) (see detailed review of solar wind streams by Richardson, 2018).

There are also more explosive events happening at the surface of the Sun, such as a Coronal Mass Ejection (CME). A CME is a massive explosion of plasma that spews out a large cloud of plasma and magnetic field, which propagates outward through the solar system. The resulting solar wind structure, the Interplanetary CME (ICME), interacts with the slower solar wind in front of it. The large difference in speed creates a shock front in front of the ICME cloud, which can accelerate plasma to MeV energies. These accelerated particles are called Solar Energetic Particles (SEPs). As the ICME propagates outward it evolves; it stretches out both radially and longitudinally, decelerates, its density and magnetic field magnitude decreases and its shock (if there is one) evolves (e.g. Grison, Benjamin et al., 2018; Lindsay et al., 1999; Savani et al., 2011; Wang et al., 2005). At Venus, the ICMEs will interact with the induced magnetosphere. The interaction with an ICME, as well as a CIR, causes large disturbances in the Venusian plasma environment (e.g. Edberg et al., 2011; Futaana et al., 2008), and may even cause a 100-fold increase in the escape (Luhmann et al., 2006). This interaction is further discussed in subsection 7.4.1.

2.3 The Venusian Induced Magnetosphere

As Venus does not have a strong intrinsic magnetic field, the solar wind reaches directly to the upper atmosphere of Venus, which forms an obstacle to the solar wind: the induced magnetosphere (see detailed reviews by e.g. Futaana et al., 2017; Luhmann, 1986; Russell, 1991). As the upper atmospheric particles are ionised, they mass load the solar wind and slow it down. In front of the obstacle the IMF, frozen into the solar wind flow, piles up. The magnetic field in the undisturbed solar wind continues past the obstacle, and the magnetic field lines are stretched around the obstacle, which forms the Venusian magnetotail, as shown in Figure 2.2. Upstream of the obstacle, where the solar wind is slowed

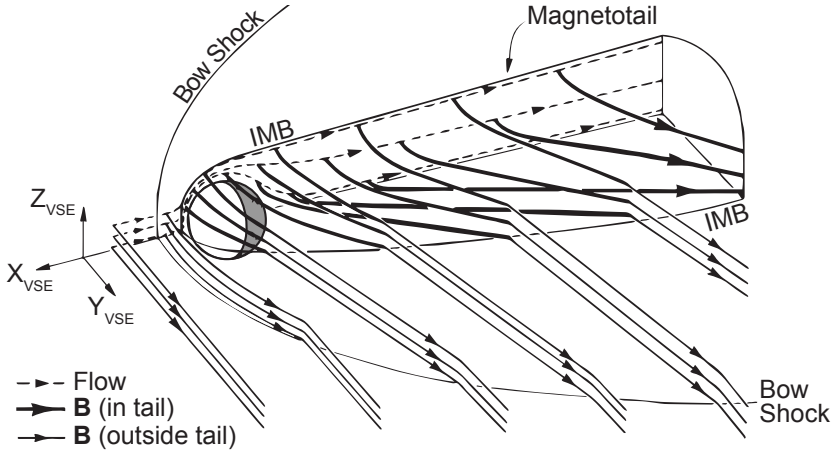


Figure 2.2: The induced magnetosphere of Venus, formed by the interaction between the solar wind and an unmagnetized object with a conductive ionosphere. See the text for more details (adapted from Saunders and Russell, 1986).

down from supersonic to subsonic speeds, a bow shock is formed. The region between the induced magnetosphere and the bow shock is the magnetosheath, which contains the slowed down and heated solar wind plasma that is forced to move around the induced magnetosphere of Venus.

In addition to the piled up IMF in front of Venus, the IMF induces currents in the conductive ionosphere. The current further induces a magnetic field to prevent the diffusion of the IMF into the atmosphere. The superposition of the induced magnetic field and the piled up IMF forms the so called magnetic pileup region around the obstacle. At the magnetic pileup region, most prevalent in the subsolar region, the magnetic pressure dominates and the dynamic pressure is equal to the magnetic pressure. From this interaction, a solar wind void is formed, the induced magnetosphere, and the outer boundary is commonly named the Induced Magnetosphere Boundary (IMB, see Figure 2.2). Below the magnetic pileup region, the thermal plasma pressure becomes the strongest part, and the magnetic field is equal to the thermal plasma pressure. This boundary is commonly named the ionopause. Although there are many definitions of the ionopause (Luhmann, 1986), in this thesis the described definition is used. This transition can be expressed by the equality of pressures between the different regions

$$\underbrace{\frac{1}{2}\rho_{sw}v_{sw}^2\cos^2\theta}_{\text{Dynamic pressure}} = \underbrace{\frac{B^2}{2\mu_0}}_{\text{Magnetic pressure}} = \underbrace{nkT_e}_{\text{Thermal pressure}} \quad (2.5)$$

where ρ_{sw} and v_{sw} is the solar wind mass density and speed, respectively, θ is the angle between the boundary normal vector and the solar wind velocity vector, B is the magnetic field strength, here of the pileup region, μ_0 is the permeability in vacuum, n is the density in the ionosphere, k is Boltzmann's constant, and T_e is the temperature of electrons in the ionosphere.

The most common description of the induced magnetosphere is expressed through Equation 2.5. However, Venus has two different states of the ionosphere: the magnetized and unmagnetized states. The above description is valid for the unmagnetized state, where there are no large scale magnetic fields inside the ionosphere, only small scale fields, sometimes denoted flux ropes (Russell and Elphic, 1979). In this state, the ionopause is well defined, and the magnetic pressure is clearly compensated by the thermal plasma pressure, as shown in Figure 2.3a. On the other hand, in the magnetized state, the thermal plasma pressure cannot compensate for the solar wind dynamic pressure and the magnetic fields seem to convect downwards and dissipate into the ionosphere. In this case, the ionopause becomes thicker and the pressure is gradually changed from dominated by magnetic pressure to thermal pressure, as in Figure 2.3b and c. In addition, large scale magnetic fields are present down to a few hundred km's into the ionosphere. Normally, the unmagnetized state is found near the subsolar point, evident from PVO measurements (Luhmann and Cravens, 1991), while in the polar region, measured by VEx, the ionosphere is more frequently magnetised (Angsmann et al., 2011).

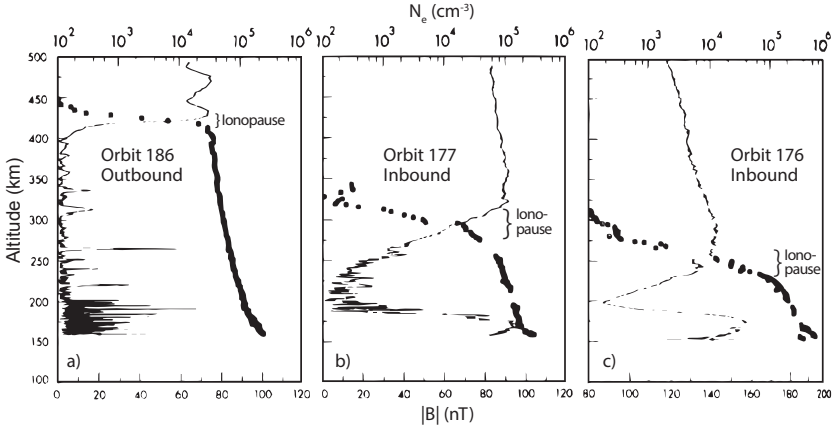


Figure 2.3: Electron density and magnetic field strength profiles measured in the ionosphere of Venus from three different orbits of the PVO mission (adapted from Elphic et al., 1981).

The interaction between the solar wind and the Venusian atmosphere causes the escape of atmospheric particles to space. This is evident in part by the presence of planetary plasma, mostly O^+ , in the magnetotail. The escape

channels, and their importance for Venus is described in chapter 3. In addition to planetary plasma, the magnetotail also contains some solar wind plasma, meaning that the solar wind is capable of penetrating into the magnetotail (e.g. Fedorov et al., 2011; Jarvinen et al., 2013).

The typical range of ion and electron energies in the different plasma regions of Venus is included in Figure 1.1. A typical measurement of an orbiting spacecraft passing through the different plasma regions will be shown in Figure 4.3, and is further explained in section 4.3.



3. Atmospheric Escape

The escape of atmospheric particles to space is one of the most important processes for understanding the evolution of planetary atmospheres. There are several different processes responsible for the escape of atmospheric particles, and the processes depend highly on the type of interaction the solar system body has with the solar wind. This section summarises the escape processes that has, or had, a significant impact on the Venusian atmospheric evolution.

In order for a particle to escape to space, from a body with a gravity force, it needs to reach above the escape velocity. The escape velocity v_{esc} is found from the conservation of energy, where the kinetic energy K of the particle is, at least, equal to the work W needed to reach an infinite distance from the body,

$$K + W = 0, \quad (3.1a)$$

$$\frac{mv_{esc}^2}{2} - \frac{GMm}{r} = 0, \quad (3.1b)$$

$$v_{esc} = \sqrt{\frac{2GM}{r}}, \quad (3.1c)$$

where m the mass of the escaping particle, r is the distance from the centre of mass of Venus, G is the universal gravitational constant, and M is the mass of Venus. At the surface the escape velocity of Venus is 10.36 km/s.

The most common atmospheric particles to escape from Venus is hydrogen and oxygen, and their ion counterparts (e.g. Barabash et al., 2007a; Vaisberg et al., 1995). This is a consequence from the composition of the upper atmosphere of Venus, which is mainly O^+ , O and H (see Figure 2.1). When discussing the escape of these species we may use the escape energy instead of the velocity.

The energy is dependent on the mass of the species as $E = mv^2/2$, and the escape velocity of 10.2 km/s near the exobase at ~ 200 km altitude gives 8.67 eV for O and 0.54 eV for H.

3.1 Thermal Escape

3.1.1 Jeans' Escape

The neutral atoms near the exobase can be assumed to have a Maxwell-Boltzmann velocity distribution $f(v)$. Particles populating the high-energy tail of the velocity distribution, above the escape velocity, can escape the planet if they are directed upward, as collisions are negligible above the exobase (Jeans, 1925). The escaping flux through Jeans' escape Φ_{Jeans} [$\text{m}^{-2} \text{s}^{-1}$] is calculated through an integration of the distribution over the velocities above escape velocity v_{esc} (Catling and Kasting, 2017)

$$\Phi_{Jeans} = \frac{n}{4} \int_{v_{esc}}^{\infty} f(v) v dv. \quad (3.2)$$

However, as the neutral atoms velocity distribution is truncated at the escape velocity, the particles strictly do not have a Maxwell-Boltzmann distribution near the exobase. Monte Carlo simulations have indicated that the Jeans' escape from Equation 3.2 may be overestimated by $\sim 30\%$ (e.g. Chamberlain, 1963; Pierrard, 2003).

In the Venusian atmosphere before 3.9 Ga, the heating from the solar radiation and the large amount of water in the atmosphere presumably increased the upper atmospheric temperatures (e.g. Erkaev et al., 2013; Johnstone et al., 2018). A higher temperature would have pushed a larger portion of the distribution above the escape velocity. Therefore, a large amount of hydrogen could potentially have escaped from the Venus early atmosphere through Jeans' escape. Oxygen atoms, on the other hand, are too heavy to reach above the escape velocity by heating processes, and did not escape the atmosphere through Jeans' escape (Kasting and Pollack, 1983).

At present-day Jeans' escape is not an important process for the escape of Venusian atmospheric constituents. It is estimated that hydrogen escapes at a rate of $2.5 \cdot 10^{19} \text{ s}^{-1}$ (compare with other rates in Table 3.1 and Table 3.2), while oxygen is too heavy for it to escape at any important fraction (Lammer et al., 2006).

3.1.2 Hydrodynamic Escape

If there is a considerable heating of the upper atmosphere from solar radiation, a significant portion of the lighter particles in the upper atmosphere may reach above escape velocity simultaneously. When this happens, the upper atmosphere will move away from a hydrostatic regime and dynamically expand outwards.

This leads to a significant escape of lighter particles to space. In addition, a significant portion of heavier particles may escape due to drag forces exerted on them from the expanding lighter particles. This type of escape is denoted hydrodynamic escape, or atmospheric blow off.

For Venus, hydrodynamic escape was presumably a very important process before 3.9 Ga, when the solar EUV radiation was much stronger (e.g. Tu et al., 2015). The atmosphere was significantly more heated and expanded, inducing a hydrodynamic escape from which a large portion of the hydrogen, mostly originating from the water, left Venus. A portion of heavier constituents, such as oxygen, presumably escaped due to the drag forces, but not to a significant degree (e.g. Chassefière, 1996; Gillmann and Tackley, 2014; Kasting and Pollack, 1983; Wordsworth and Pierrehumbert, 2013).

Today, the CO₂ emissions cool the upper atmosphere leading to low thermospheric temperatures, which prevents an atmospheric blow off (e.g. Lammer et al., 2006; Tian, 2009). Therefore, this process is not in operation for the present Venus.

3.2 Non-thermal Escape

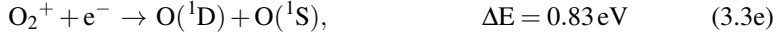
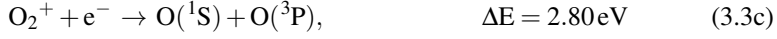
The loss of atmospheric particles through non-thermal escape is mostly concerned with ionised particles which are accelerated by either electromagnetic forces generated from the solar wind interaction, or by pressure gradients. The acceleration can be described either through a kinetic view, where the particles are treated as test particles in background fields, accelerated by the Lorentz force (Equation 3.6), or by an MHD approach using the momentum equation (Dubinin et al., 2011; Futaana et al., 2017). The two approaches are used under different circumstances. In the case of dominating solar wind density, the kinetic view can be used, while if the density of the planetary particles is close to equal to the solar wind density, the MHD approach should be used to account for the effects of the planetary particles on the electromagnetic fields. In the following subsections different processes of non-thermal escape is described, and how important they are, or were, for the Venusian atmospheric evolution.

3.2.1 Photochemical Reactions

There are a number of chemical reactions occurring in the upper atmosphere that are exothermic, where the excess energy is released and given to the reactive particles in the form of kinetic energy. This excess kinetic energy may lead to the escape of the particles, if the particles reach above escape energy and is directed outward from the planet. In general, the chemical reactions occurring in the Venusian upper atmosphere provides energies of several 0.1 eV to <10 eV (Lammer, 2013).

For Venus, the chemical reactions that provide the highest kinetic energy to

oxygen atoms is dissociate recombination of O_2^+ (Fox and Hać, 2009)



As none of the chemical reactions provide energies above the escape energy for O of 8.67 eV, it does not lead to atmospheric escape. On the contrary, for H there are several reactions that lead to kinetic energies above the escape energy of 0.54 eV (Lammer et al., 2006)



Today, the escape of H through photochemical reactions is around $(3 - 8) \cdot 10^{25} \text{ s}^{-1}$, estimated from both measurements by PVO and modelling results (Donahue and Hartle, 1992; Lammer et al., 2006), which is a significant rate and need to be taken into account for the total escape of H.

Even if the energy provided by the photochemical reactions does not lead to the escape of atmospheric constituents, the energy can put the particles on ballistic trajectories. These ballistic particles will travel far out from the planet, although still gravitationally bound, and create a “hot corona” of both H and O. Some may reach altitudes above the IMB. If the particles outside the IMB are ionised, they will interact directly with the solar wind and become pickup ions, which is further discussed in next subsection (3.2.2).

3.2.2 Pickup ions

If the neutral particles that are gravitationally bound to Venus, but outside of the induced magnetosphere, are ionised, they will be exposed to the solar wind or magnetosheath plasma. These particles can be ionised through EUV radiation or charge exchange with the solar wind particles



The charge exchange process is valid for both planetary oxygen and hydrogen. As neutral particles they are not affected by the electromagnetic fields of the solar wind, but as soon as they are ionised they are accelerated by the Lorentz force

$$\vec{F} = q \left(\vec{E} + \vec{v} \times \vec{B} \right), \quad (3.6)$$

where q is the ion charge, \vec{E} is the electric field, \vec{v} is the velocity, and \vec{B} is the magnetic field. These pickup ions are treated by a kinetic approach of test particles in the background solar wind fields, where the electric field \vec{E} is the solar wind convective electric field $\vec{E}_{\text{conv}} = -\vec{v}_{\text{sw}} \times \vec{B}_{\text{IMF}}$.

The pickup of planetary ions by the solar wind is a common process at Venus. These ions form a “plume” structure in the solar wind $+E$ hemisphere. The ions are accelerated to solar wind speeds and escape from the Venusian atmosphere through the magnetosheath (e.g. Luhmann et al., 2006; McEnulty et al., 2010). In the $-E$ hemisphere, the accelerated ions may move back towards the atmosphere, which can also occur if the gyroradius is on the scale of the planetary radius.

The total escape from pickup ions today is estimated from modelling results as $1 \cdot 10^{25} \text{ s}^{-1}$ for both H^+ and O^+ (Lammer et al., 2006), which agrees with results of the PVO missions of $1 \cdot 10^{25} \text{ s}^{-1}$ for O^+ (Luhmann and Bauer, 1992). However, Venus Express measurements show that only about $(2 - 5) \cdot 10^{23} \text{ s}^{-1}$ of O^+ escapes in the magnetosheath, corresponding to $\sim 30\%$ of the total net escape of O^+ from Venus (Masunaga et al., 2019).

3.2.3 Atmospheric Sputtering

An ion or neutral particle, accelerated back towards the atmosphere, may act as a sputtering agent. The agent will collide with particles in the atmosphere and transfer energy to the atmospheric particles. The collision may also lead to ionisation or excitation of neutral particles. The atmospheric loss from sputtering is dependent on the amount of energy transferred to the atmospheric particles, either through collisions with the sputtering agent or a cascade of collisions initiated by the sputtering agent, and on how much energy is needed for the particle to escape (Lammer, 2013).

Unfortunately, there are to this date no direct measurements of this process and how large escape of O it causes for Venus. Nevertheless, modelling shows that it can cause the escape of as much as $6 \cdot 10^{24} \text{ s}^{-1}$ or 25% of the total modelled O^+ escape from Venus (Lammer et al., 2006; Luhmann and Kozyra, 1991). Therefore, sputtering is potentially the largest source of neutral O escape. The escape from sputtering is insignificant for neutral H, as there is a much lower amount of H in the source region for sputtering, around the exobase, at Venus (see density profiles in Figure 2.1).

3.2.4 Magnetotail escape - Momentum transfer, Cold Plasma Outflow and Plasma Instabilities

There are several non-thermal processes that lead to the escape of ions through the magnetotail. From the measurements made in the magnetotail, it is not straightforward to separate which process is responsible for each ions escape. Therefore, several of the processes that are likely responsible for the majority of the ion escape through the magnetotail is described altogether in this subsection.

When the fast solar wind plasma flows around the induced magnetosphere it interacts with the cold ionospheric plasma and transfer some of its energy and momentum, as described in section 2.1. This additional energy and momentum transferred to the ionospheric plasma can partly explain the high velocities above the exobase in the terminator region. If the energy and momentum provides a velocity above the escape velocity, the ions can escape through the magnetotail and along the IMB (Dubinin et al., 2011; Lundin et al., 2007; Pérez-de-Tejada et al., 2011). The energy and momentum transfer from the solar wind is dependent both on the available energy in the solar wind, and in the size and variations of the interaction area.

Because the IMF is closely draped around the planet and stretches out on the nightside, two lobes of opposite magnetic field polarity are formed in the magnetotail. In between the lobes there is a region, the plasma sheet, with a significant plasma acceleration from the $\vec{j} \times \vec{B}$ force (2nd term in Equation 2.2). Here, the majority of the planetary plasma is accelerated downstream in the tail (Nilsson et al., 2012) and escape the planet (Barabash et al., 2007a). In the plasma sheet there are also indications of reconnection events (Zhang et al., 2012), common for magnetospheres formed by strong intrinsic magnetic fields, which transforms magnetic energy to kinetic energy and can provide further acceleration of plasma downstream from Venus. The reconnection can also provide bursty flows of plasma back towards Venus, return flows. Measurements from VEx indicate a significant presence of return flows in the magnetotail that can affect the net escape rates (Kollmann et al., 2016), which could be explained by reconnection events (see section 6.2). However, the detailed physics of the return flows is not yet fully investigated.

An energisation of the plasma can lead to the upflow of electrons, which are lighter than ions and more receptive to acceleration against the gravity. As the electrons move upward and leave the ions behind the charge separation form a polarisation, or ambipolar, electric field (3rd term in Equation 2.2). The polarisation electric field will accelerate the ions towards the electrons, to remove the charge separation, leading to the upflow of ions. If the electric field is strong enough, it can lead to the escape of ionospheric constituents. Measurements from VEx have shown that an electric field as strong as 9.9 ± 1.1 V can be formed in the Venusian upper ionosphere (Collinson et al., 2016), which is strong enough to accelerate O^+ ions to above escape energy.

PVO measured the presence of detached plasma clouds in the magnetotail of Venus. The detached plasma clouds are temporal bubbles of high plasma

density and magnetic field strength (e.g. Brace et al., 1982; Russell et al., 1982) mainly located near the boundary region of the magnetotail. It is suggested that the shear between the fast solar wind stream outside the boundary and the slower ionospheric plasma inside the boundary can cause a Kelvin-Helmholtz instability, which could result in detached plasma clouds of ionospheric origin. The total escape from the plasma clouds depends on the frequency of which they are formed, and how large the clouds are, but is estimated from modelling to be around $(5 - 10) \cdot 10^{24} \text{ s}^{-1}$ (Lammer et al., 2006) and from PVO measurements on the order of $2 \cdot 10^{25} \text{ s}^{-1}$ (Russell et al., 1982).

The total escape rates in the magnetotail, as a consequence of the abovementioned processes, have been determined from both PVO and VEx measurements. Some discrepancies between the two missions still exist. The PVO measurements indicate escape on the order of $(6 - 50) \cdot 10^{24} \text{ O}^+ \text{ s}^{-1}$ (Brace et al., 1987; McComas et al., 1986), where the upper boundary is likely overestimated by a factor 5 due to assumptions in the calculations (Fedorov et al., 2011). The VEx measurements indicate an escape rate of $(3 - 6) \cdot 10^{24} \text{ s}^{-1}$ (see review by Futaana et al., 2017), which is lower than those of PVO. The ambiguity may be explained by the difference in upstream parameters during the PVO and VEx era, where e.g. the solar maximum during PVO was much stronger than the solar maximum during VEx era (see Figure 1.1). In this thesis, the VEx measurements of the escape rates and the dependence on the upstream solar wind parameters are used to try to explain the difference between the VEx and PVO results of the O^+ escape rates (see section 6.3).

The H^+ ion escape through the magnetotail has only been measured by VEx, and studied only during solar minimum. The escape rates for H^+ was found as $7 \cdot 10^{24} \text{ s}^{-1}$ (Fedorov et al., 2011), and is escaping at a ratio with O^+ ion escape of $Q_{\text{H}^+}/Q_{\text{O}^+} = 1.9 - 2.6$ (Barabash et al., 2007a; Fedorov et al., 2011), which means that it escapes at a ratio near the stoichiometric ratio of water of 2:1. This is an important finding, since it is directly related to the escape of water from Venus. In this thesis, the ratio of the escape of O^+ and H^+ is further investigated, and discussed in section 6.1.

3.3 Summary of Measured Escape Rates at Venus

The escape rates from the different escape processes related to Venus is summarised in Table 3.1 for oxygen and in Table 3.2 for hydrogen. As there are many studies that have investigated the escape from Venus, the escape rates show a large variety and range. It is challenging to compare the numbers with each other due to the large variety of methods used to determine them. For example, the escape rates found through modelling is dependent on the input parameters and the inner boundary condition (ionosphere). As mentioned above, there is a difference between the time periods of PVO and VEx, where the escape rates measured by PVO were generally higher than those measured by VEx. Most of the modelling work before 2007 used constraints found from

PVO, meaning that a direct comparison between the modelling results and those of VEx cannot be done. Instead, an estimation of the fraction of the total net escape rate for each process may be used.

A clear outcome of the summarised tables is that the main escape channel for oxygen is through ion escape in the magnetotail. Therefore, this part is the most important to determine in order to evaluate the effect on the atmospheric evolution from the atmospheric escape to space. The ion escape through the magnetotail is also the main topic of this thesis. The results of the studies of the escape rates are summarised in chapter 6.

Table 3.1: Summary of the reported escape rates for each escape processes for O and O⁺ at Venus today and their fraction of the total net escape (described in section 3.1 and 3.2) from both modelling and in situ measurements.

	Escape process O ⁺ and O	Escape rate (10 ²⁴ s ⁻¹) modelling in situ meas.	Fraction of total net escape
Thermal escape	Jeans' Escape	-	0.0
	Hydrodynamic Escape	-	0.0
Non-thermal escape	Photochemical reactions	-	0.0
	Pickup ion	10 ^a	0.1-0.5
	Sputtering	6 ^{ad}	<0.3
	Magnetotail escape ^a	5-10 ^a	0.4-0.8
Total escape escape		20-26 1-50	1.0

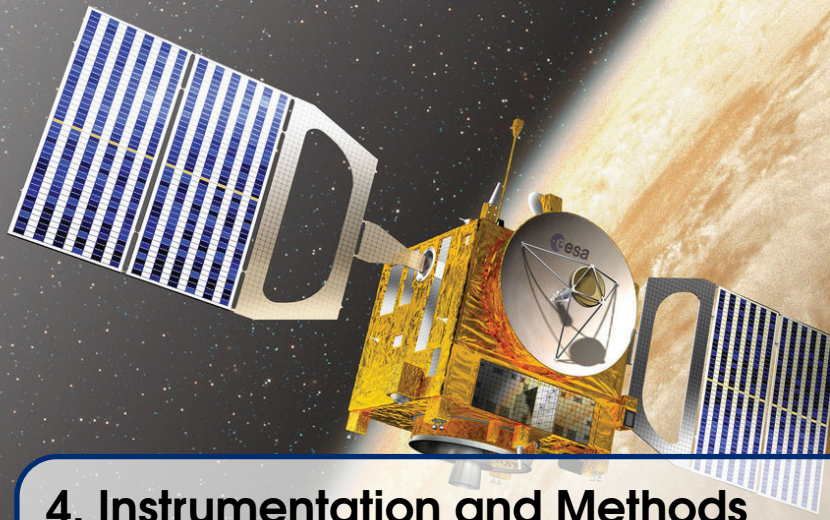
^aLammer et al. (2006)
^bLuhmann and Bauer (1992)
^cMasunaga et al. (2019)
^dLuhmann and Kozyra (1991)
^eMcComas et al. (1986)
^fBrace et al. (1987)
^gFedorov et al. (2011)
^hFutaana et al. (2017)

Table 3.2: Summary of the reported escape rates for each escape process for H and H⁺ at Venus today, same structure as Table 3.1.

	Escape process H ⁺ and H	Escape rate (10 ²⁴ s ⁻¹) modelling in situ meas.	Fraction of total net escape
Thermal escape	Jeans' Escape	0.000025 ^a	0.0
	Hydrodynamic Escape	-	0.0
Non-thermal escape	Photochemical reactions	30-80 ^a	<0.5
	Pickup ion	10 ^a	<0.3
	Sputtering	-	0.0
	Magnetotail escape	<70 ^a	>0.5
Total escape escape		<128	1.0

^aLammer et al. (2006)

^bFedorov et al. (2011)



4. Instrumentation and Methods

4.1 Venus Express

The Venus Express (VEx) spacecraft was launched in November 2005 and arrived at Venus in April 2006. It was operated in orbit around Venus for ~ 8.5 years until November 2014 when it shut off due to lack of fuel, and incinerated in the atmosphere in January 2015. The mission was designed to make a comprehensive study of the Venus atmosphere, plasma environment, and surface physics. VEx was developed in a short time as five out of the seven included instruments were inherited from the earlier Rosetta and Mars Express missions, and the spacecraft structure was a copy of the Mars Express spacecraft, with improvements to operate in the Venusian space environment (Svedhem et al., 2007).

With an elliptical orbit of 24 hours VEx reached more than 3000 orbits around Venus during its lifetime. The nominal pericentre was located at 250 km, close to the North Pole, and the apocentre at 66 000 km ($\sim 11 R_V$). In addition, the mission made several atmospheric drag experiment campaigns between 2008-2013 where the pericentre was lowered to 160 km. Furthermore, during the summer of 2014, an aerobraking campaign was executed, with a pericentre lowered to ~ 130 km for several consecutive orbits.

4.2 MAG

The magnetometer instrument package on board Venus Express, MAG, was composed of a pair of ring-coil fluxgate magnetometers. One was mounted on a short boom and the other on the spacecraft body, to be able to subtract the magnetic noise from the spacecraft. MAG had several modes with frequencies of 1, 32, and 128 Hz, to be executed in the different plasma domains near

Venus (Zhang et al., 2007). In this thesis, the 4 s averaged data is used (Level-3 data in ESA Planetary Science Archive (PSA)), which was handled with care by the PI team (IWF in Graz, Austria) to remove the known noises and operation-related issues. As we are interested in the average magnetic field during the 192 s measurements by IMA (see section 4.3), this resolution is sufficient.

4.3 ASPERA-4/IMA

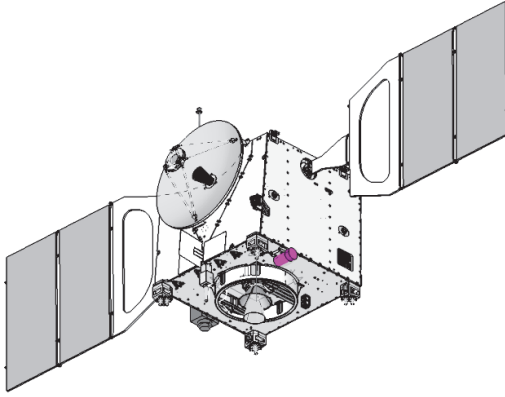


Figure 4.1: The Venus Express spacecraft structure, with the location of IMA shown (magenta color) (copyright: IRF).

The plasma instrument package on board VEx, the Analyser of Space Plasmas and Energetic Atoms (ASPERA-4), was built by a consortium led by the Swedish Institute of Space Physics/Institutet för Rymdfysik (IRF) in Kiruna, Sweden (Barabash et al., 2007b). The instrument package comprised four instruments. The main unit included the Electron Spectrometer (ELS), the Neutral Particle Imager (NPI), and the Neutral Particles Detector (NPD), while the Ion Mass Analyser (IMA) was a separate unit. For this thesis work, only the measurements made by the IMA instrument is used, which location on the spacecraft is

shown in Figure 4.1 and a picture of the flight model is shown in Figure 4.2b.

The IMA instrument was a top-hat electrostatic ion spectrometer. The design was developed from the ICA and IMA instruments on board the Rosetta and Mars Express spacecraft, respectively. The schematics and a picture of the flight model is shown in Figure 4.2. Sample trajectories of ions passing through the ion optics is shown in Figure 4.2a. The first part the ion encounters is the elevation angle filter (1., numbers refer to Figure 4.2), which is composed of two deflector plates with a voltage difference between them ($\Delta U = U_2 - U_1$). The voltage is stepped through 16 steps to allow positive ions to enter at angles between $\pm 45^\circ$ with a resolution of 5.6° for each step. The second part is the electrostatic analyser (2.) which filters the ions based on their energy per charge. An electrostatic field is produced between the two plates by setting a voltage difference ($\Delta U = U_4 - U_3$). By stepping through the voltage difference, ions with different energies can enter the instrument. 96 energy steps allowing energies of 0.01-36 keV were defined, with a resolution of $\Delta E/E = 7\%$. After exiting

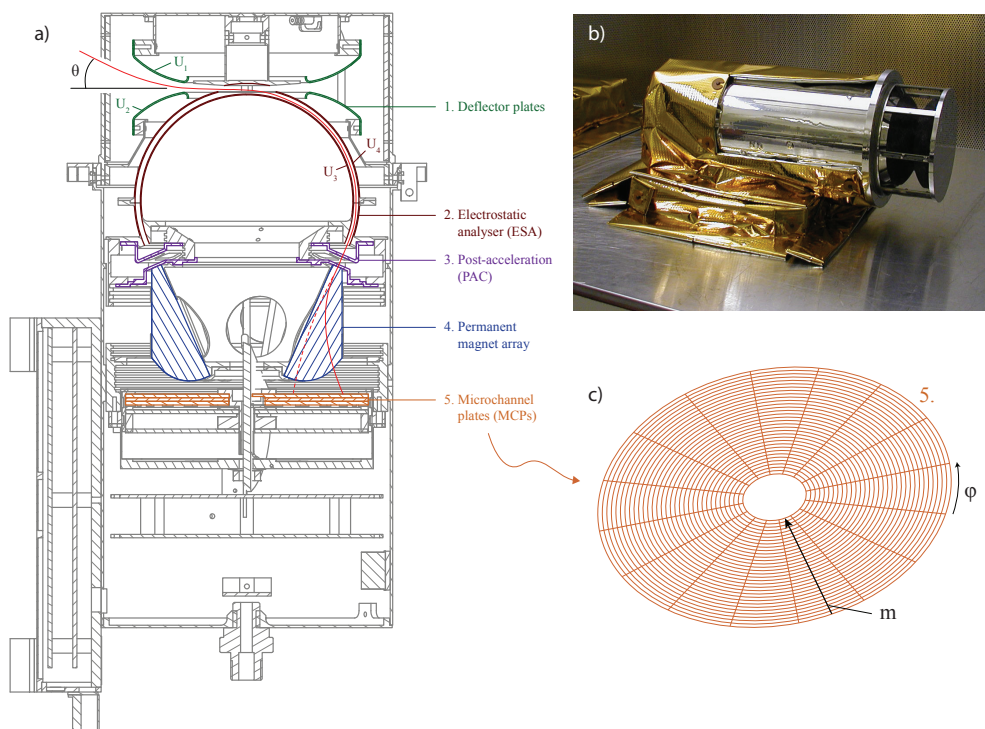


Figure 4.2: a) A schematics of IMA shown as a cut-through along the symmetry axis. Each part of the ion optics are shown with different colors, numbering used in the description in the text, b) A picture of the Flight Model (FM), and c) Schematic of the MCPs with the 32 mass rings providing the mass dimension m , and the 16 sectors in the azimuthal direction ϕ (Copyright: IRF).

the electrostatic analyser the ions are post-accelerated (3.), before entering the assembly of permanent magnets (4.). The post-acceleration was usually set to the highest setting of 3650 V. The magnetic assembly (4.) provides a cylindrically symmetric magnetic field, in which the ions' trajectories are determined by their momentum per charge, or gyroradius $r_L = (mv_{\perp}/|q|B)$, where v_{\perp} is the velocity perpendicular to the magnetic field B , and q is the charge. As the energy per charge is already determined, the only difference between the ions at this point is their mass per charge. Heavier ions have a larger gyroradius and follow the dashed red trajectory in Figure 4.2, while the lighter ions have a shorter gyroradius and ends up nearer the outer edge of the multichannel plates (MCPs) (5.). The MCPs are divided into 32 mass channels that records the radial position of the ions, which starts from the centre and counts outwards, while the mass is in the opposite direction as indicated in Figure 4.2c. In addition, the MCPs are divided into 16 sectors of 22.5° each,

which records the azimuthal direction the ions had when entering the instrument. Therefore, the total field-of-view (FOV) of the instrument is $90 \times 360^\circ$. The full scan of all energy levels, for each elevation angle, is provided in 12 s, which with the full elevation sweep of 16 steps leads to a full scan in 192 s. For more details on the instrument design see Barabash et al. (2007b).

An example of the ion characteristics measured by IMA during one pericentre passage of VEx is shown in Figure 4.3. The calibrated positions of the different ion mass per charges for the lower energies are shown by the white lines in Figure 4.3c and d. Note that the energy is corrected for an offset in the energy table and the spacecraft charging in this figure, in order to provide adequate measurements of the ions inside the ionosphere of Venus (see subsection 4.3.1 for more details on the correction). In addition, as the instrument is placed on a spacecraft body, a part of the FOV is blocked by the spacecraft body and solar arrays, which is shown in Figure 4.3d and f with a black wire frame. Furthermore, the FOV does not cover the full 4π sr sphere ($180 \times 360^\circ$). Therefore, there is a need for accounting for the potential loss of parts of the ion distributions in the measurements. In this thesis, average velocity distributions are used to counteract this issue. The method of creating these average velocity distributions is further described in subsection 4.4.2.

4.3.1 Energy Table Corrections for Low Altitude Measurements

It is known that an undetermined offset in the high voltage supply is a source of an ambiguity of the energy table. This is represented as an offset in the available IMA energy tables. The effect is seen as an apparent higher measured speed (~ 20 km/s) of the ions in the Venusian ionosphere compared to the ram speed of the spacecraft (~ 7 -8 km/s) and the results of previous measurements of ion velocities in the ionosphere by PVO (2-5 km/s near equatorial exobase, Knudsen et al., 1980). IMA was not designed to measure ionospheric ions (Barabash et al., 2007b) and thus, we empirically re-calibrated the energy table using available ionospheric IMA measurements.

In the collisional plasma below the exobase, the dynamics of the cold ionospheric plasma is mainly driven by collisions with the neutral atmosphere. Therefore, the bulk velocity for all species are assumed to be the same. Three ion species are observed in the ionospheric measurements of mass per charge 1 (H^+), 4 (He^+), and 16 (O^+) (see Figure 4.3c). As their bulk velocity in the spacecraft frame is assumed to be the same, their energy per charge differ only by their mass per charge. Therefore, the energy offset of IMA can be calculated from a set of three equations for the ions energies (see supplementary material to Persson et al., 2019, paper II). The energy offset was calculated to -16.7 eV, and resulted in a velocity of the ions in Figure 4.3c of 9.6 km/s. The velocity difference between the measured ions and the spacecraft velocity provides the velocity of the ions in the ionosphere of Venus. The results of the measured ion velocities in the ionosphere of Venus are summarised in chapter 5.

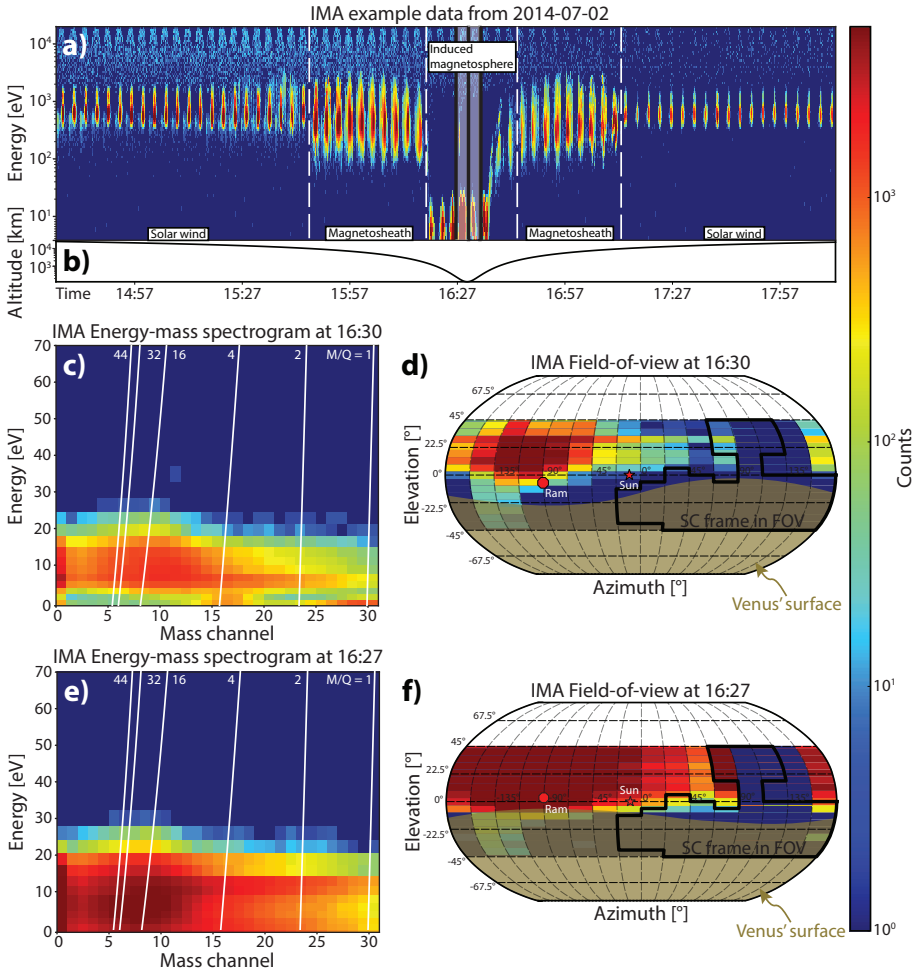


Figure 4.3: Example IMA data from one pericentre passage of VEx on July 2, 2014. a) Energy-time spectrogram of ions. The plasma domains which VEx passed through are indicated with the white dashed lines. The grey areas at 16:27 and 16:30 are the full 192 s scans of IMA which are used in (c, d) and (e, f), respectively. c) and e) shows the energy-mass spectrograms, integrated over all directions, where the white lines show the calibrated positions of six different mass per charges. d) and f) show the FOV of the data, integrated over energy and mass. The black wire frame shows the maximum blocking direction by the spacecraft body and solar arrays, the red circle shows the ram direction for this time, the red star the location of the Sun in the IMA FOV, and the solid dark yellow area indicates the Venusian surface as seen by IMA. The colour scale shows the ion counts per pixel. Adapted from Persson et al. (2019, paper II). Note that the energy table here is corrected for an offset, described in subsection 4.3.1.

4.3.2 Mass Separation of Heavy Ions

The IMA instrument has moderate mass separation capabilities. This means that it is relatively easy to separate the heavier and lighter elements, such as H^+ , He^+ , He^{++} , and heavy ions, in the data. However, to separate the heavier ions from each other, mainly O^+ , O_2^+ , and CO_2^+ (the most common heavy ions in the Venusian ionosphere, see Figure 2.1, e.g. Fox and Sung, 2001; Taylor et al., 1980), a detailed study is needed. From the IMA instrument on board Mars Express it was shown that it is possible to separate the O^+ , O_2^+ , and CO_2^+ through using a Gaussian fitting scheme (Carlsson et al., 2006, example in Figure 4.4a). Therefore, an analysis of a possible mass separation of the heavier ions on a statistical basis was conducted.

The calibration of the instrument showed that each species will give a Gaussian shape over the mass channels in the instrument MCPs. This Gaussian shape can be used to make statistical fits over the mass channels in order to extract each of the species from the data. Therefore, the O^+ , O_2^+ , and CO_2^+ species can be found by fitting three Gaussians to the heavy ion peak from the measurements. The position of the Gaussian was estimated empirically from calibration data (white lines in Figure 4.3), and the width and height of the Gaussian is fitted to the data by using a least square method. As the exact position of the species for energies below 100 eV could not be found from calibration (as it is not feasible to produce an ion beam of so low energies in a calibration lab) the locations was found from in-flight calibration, and the fitting scheme used here allowed some small movements of the position.

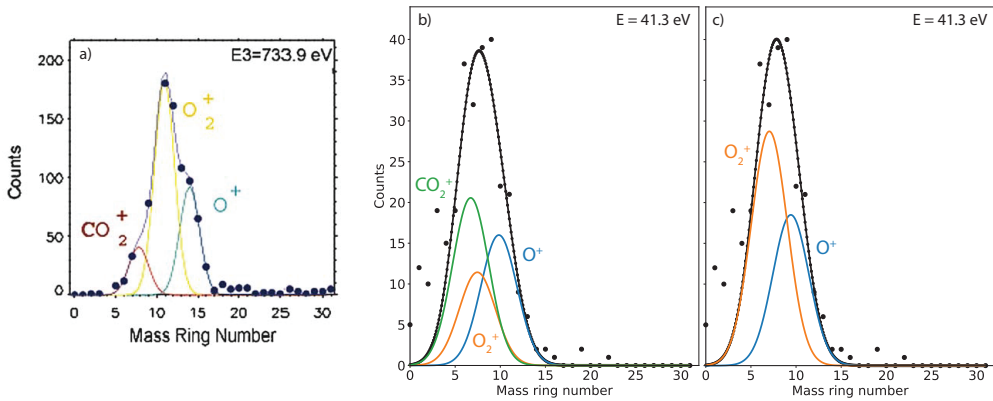


Figure 4.4: a) Mass composition analysis on data from IMA on Mars Express (Carlsson et al., 2006), b) mass composition analysis on data from IMA on Venus Express using three Gaussian peaks, c) same as b) but with only two Gaussian peaks.

An example of fitting by three Gaussian distributions is shown in Figure 4.4b. Although it is technically possible to make such a fit with the three Gaussian

distributions, the results are very sensitive to the initial guess of the fit and how much the fitting scheme is allowed to vary the three parameters. The fitting results show a tendency to overestimate the contribution of CO_2^+ , which should be the minor species of the three (see Figure 2.1; Taylor et al., 1980). These signatures also vary significantly with time and orbit. We attempted to decrease the scheme to using only two peaks (Figure 4.4c), representing O^+ and O_2^+ , which dominate at altitudes above 150 km (Fox and Sung, 2001; Taylor et al., 1980). However, even with only two peaks it was realised that the fitting is still very sensitive to the initial guess. Our conclusion was that the positions of the heavy ions in the VEx/IMA measurements are not separated well enough to use a statistical method of Gaussian fits for separating the species. Therefore, in this thesis we assume that a majority of the heavy ions is O^+ , except when expected to be dominated by O_2^+ (usually < 200 km, see chapter 5).

From the analysis of the heavy ions in the ionosphere (Persson et al., 2019, paper II), it was found that the scale height might instead be an indication of the change in atmospheric composition near 150 km. The region with a lower scale height in the lowest altitudes is likely dominated by the O_2^+ ions, as was also found by PVO measurements (Taylor et al., 1980). However, as the instrument was not designed to make measurements near the ionospheric peak, the measurements are challenging to interpret at these altitudes. The signal spreads significantly in the lowest altitudes, both in energy, direction and mass, seen clearly in Figure 4.3a, e and f. These “pericentre” measurements are separated out from the rest in the results (see chapter 5). In addition, the total density of the ions measured by IMA in this high density region of the polar ionosphere is much lower than found in the equatorial region by PVO. Therefore, the absolute density data should be interpreted with significant care. Instead, the relative density and its variations with altitude is the main focus in the investigation (see chapter 5 and Persson et al., 2019, paper II).

4.3.3 Separation of Solar Wind and Planetary Protons in the Magnetotail

As the solar wind flows around the induced magnetosphere of Venus some of it will penetrate through the boundary on the nightside and end up in the magnetotail (Fedorov et al., 2011; Jarvinen et al., 2013). These solar wind protons will mix with the protons escaping from Venus through the magnetotail. Therefore, in order to calculate the total escape rate of H^+ from the measurements, the solar wind and planetary proton populations need to be separated.

It is challenging to separate the solar wind and planetary proton populations, as they have overlapping velocity distributions. Figure 4.5 shows a typical distribution of proton velocities seen when combining magnetotail and magnetosheath measurements, here taken from measurements over the volume $X_{VSO} = [-1.5, -2.5] R_V$, $R_{VSO} = [0, 3.0] R_V$. The VSO (Venus-Solar-Orbital) cartesian coordinate system is defined with X_{VSO} pointing along the Venus-Sun line, Z_{VSO} is the northward normal to the Venus orbital plane and Y_{VSO} completes the orthogonal system. The cylindrical VSO coordinate system combines

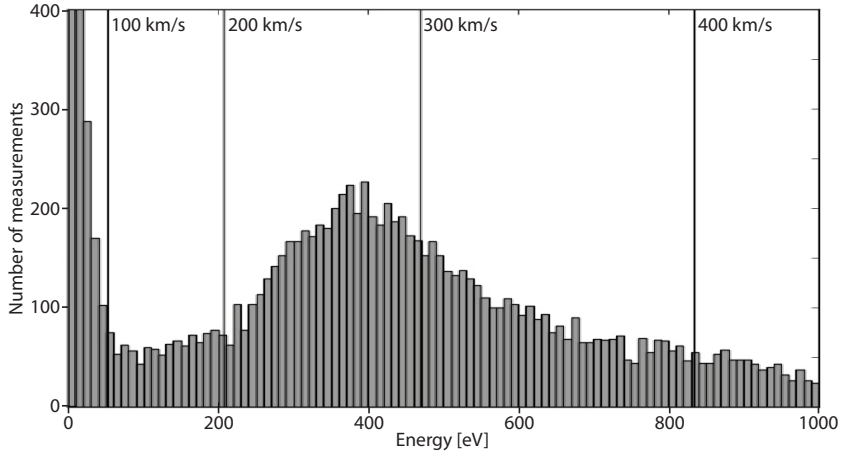


Figure 4.5: Energy distribution of protons measured in the magnetotail and magnetosheath of Venus. The vertical lines indicates the proton speed. The peak near 400 eV represent the magnetosheath proton population, while the peak near 0 eV represent the planetary proton population.

the Y_{VSO} and Z_{VSO} coordinates into the $R_{VSO} = \sqrt{Y_{VSO}^2 + Z_{VSO}^2}$, which provides the orthogonal distance from the X_{VSO} -axis. From Figure 4.5 it is clear that there are two proton populations in the magnetotail: (a) one distribution with a peak of very low energies <50 eV, originating from the Venusian atmosphere, and (b) one broad distribution with a peak near 400 eV, originating from the slowed down and heated solar wind population in the magnetosheath, which can penetrate into the magnetotail. In the magnetotail, the solar wind population may even be decelerated to low planetary energies. The planetary population has a very low energy peak, as it originates from the thermal population in the atmosphere of Venus and is accelerated outwards. As it moves outward in the magnetotail, it will be further accelerated by e.g. magnetic tension forces (2nd term in Equation 2.2, see e.g. Nilsson et al., 2012). Therefore, the solar wind and planetary populations have overlapping distributions, which makes it challenging to separate. A common method, also adapted in this thesis, is to separate at an energy level, assuming that all protons below 200 km/s originates from the atmosphere and all above originates from the solar wind (Fedorov et al., 2011). With this method, we will include a part of the solar wind distribution, but also exclude a part of the planetary population. A sensitivity analysis was conducted, where the threshold of the energy was varied. The result confirmed that these overlaps do not have a significant effect on the calculated total escape rates (Persson et al., 2018, paper I).

4.4 Calculating Ion Properties from an Ion Spectrometer

The IMA instrument intrinsically measures the flux of particles entering the instrument aperture. The output from the instrument is raw ion counts c , which can be converted to differential flux $j(E, \Omega)$ [$\text{m}^{-2} \text{s}^{-1} \text{sr}^{-1} \text{eV}^{-1}$] by using the integration period τ , geometric factor G of the instrument, and energy E for each measurement

$$j = \frac{c}{G \cdot \tau \cdot E}. \quad (4.1)$$

The differential flux can be used to calculate the ion properties, as it is related to the phase space density $f(\vec{v})$ [$\text{s}^3 \text{m}^{-6}$] through

$$f(\vec{v}) = \frac{m^2}{2Eq_e^2} j(E, \Omega), \quad (4.2)$$

where q_e here is the elementary charge used to convert the energy unit from eV to J.

The main parameters of density, velocity, and flux is then calculated through the plasma moments, defined as

$$M^k = \int f(\vec{v}) \vec{v}^k d\vec{v}, \quad (4.3)$$

where $d\vec{v} = dv_x dv_y dv_z$. The 0th moment ($k=0$) provides the density

$$M^0 = n = \int f(\vec{v}) d\vec{v}, \quad (4.4)$$

and the 1st moment provides the flux

$$M^1 = n\vec{v} = \int f(\vec{v}) \vec{v} d\vec{v}. \quad (4.5)$$

By putting Equation 4.2 into Equation 4.4, converting from Cartesian velocity space to IMA spherical energy space, and using the discrete steps of the IMA instrument we can calculate the ion density as

$$n \cong \sum_{k,l,m} \sqrt{\frac{m}{2E_m}} j(\phi_k, \theta_l, E_m) \cos \theta_l \Delta E_m \Delta \theta_l \Delta \phi_k, \quad (4.6)$$

where θ and ϕ are the elevation and azimuth angles, respectively. Similarly, we get the flux for each direction from the 1st moment (Equation 4.5) as

$$F_x = mv_x \cong \sum_{k,l,m} j(\phi_k, \theta_l, E_m) \cos^2 \theta_l \cos \phi_k \Delta E_m \Delta \theta_l \Delta \phi_k, \quad (4.7a)$$

$$F_y = mv_y \cong \sum_{k,l,m} j(\phi_k, \theta_l, E_m) \cos^2 \theta_l \sin \phi_k \Delta E_m \Delta \theta_l \Delta \phi_k, \quad (4.7b)$$

$$F_z = mv_z \cong \sum_{k,l,m} j(\phi_k, \theta_l, E_m) \sin \theta_l \cos \theta_l \Delta E_m \Delta \theta_l \Delta \phi_k. \quad (4.7c)$$

4.4.1 Correcting Measurements for the Spacecraft Velocity

As VEx travels with speeds of up to 8-9 km/s, it is important to correct the measurements for the spacecraft velocity \vec{v}_{sc} . Both the measured energy and flux of the ions need to be corrected. The energy of the ions is corrected by transforming to velocity space and correct the velocity according to

$$\vec{v}_{ion} = \vec{v}_{meas} + \vec{v}_{sc}, \quad (4.8)$$

where \vec{v}_{ion} is the velocity of the ion in the Venusian fixed reference frame and \vec{v}_{meas} is the measured velocity. The flux can be corrected for by assuming that the phase space density is the same, independent of the reference frame used. Using Equation 4.2 to transform from differential flux to phase space density we can set up an equality between the phase space density calculated from the differential flux and energy of a spacecraft in motion ($j_1(E, \Omega), E_1$) and from the differential flux and energy measured by a spacecraft without movement in the Venusian reference frame ($j_2(E, \Omega), E_2$). This gives an equation for the differential flux $j_2(E, \Omega)$ that would have been measured if the spacecraft did not move at a high speed through the Venusian plasma environment

$$f(\vec{r}, \vec{v}) = \frac{m^2}{2E_1} j_1(E, \Omega) = \frac{m^2}{2E_2} j_2(E, \Omega), \quad (4.9a)$$

$$j_2(E, \Omega) = \frac{E_2}{E_1} j_1(E, \Omega). \quad (4.9b)$$

4.4.2 Calculating Average Escape Rates

There are several methods for calculating the average escape rates of ions from IMA measurements. In this thesis, the escape rates are calculated through dividing the magnetotail into spatial bins, wherein each bin an average ion velocity distribution is calculated. The average distributions are then used to calculate the total average ion flux, which are integrated over the magnetotail to calculate the total escape rate through the Venusian magnetotail.

First, the Venusian plasma environment is divided into spatial grids in the cylindrical VSO coordinate system. It was shown that the escape rate

calculations are not dependent on the chosen coordinate system (Nordström et al., 2013), so the asymmetry along the solar wind convective electric field (\vec{E}_{conv} ; Jarvinen et al., 2013; McComas et al., 1986; Zhang et al., 2010) can safely be ignored. The number of measurements by IMA in the Venusan plasma environment in the VSO cylindrical coordinate system is shown in Figure 4.6.

Each IMA measurement has 5 degrees of freedom, two angular directions of the incoming ions, two spatial locations of the measurement in the cylindrical VSO coordinate system, and one energy (or speed). All the IMA measurements are binned into the spatial bins in the cylindrical VSO coordinate system, which are then used to calculate the arithmetic mean over the three spherical coordinates (ϕ , θ , E). Examples of the average distribution function $\bar{J}(X_i, R_j, \phi_k, \theta_l, E_m)$ over the two angles are shown in Figure 4.7.

Now, each of the spatial bins have an average distribution function from which we can calculate the average plasma parameters from.

The total flux in the X_{VSO} direction is calculated according to Equation 4.7, which with the average distribution function $\bar{J}(X_i, R_j, \phi_k, \theta_l, E_m)$ becomes

$$F_x(X_i, R_j) = \sum_{k,l,m} \bar{J}(X_i, R_j, \phi_k, \theta_l, E_m) \cos^2 \theta_l \cos \phi_k \Delta \phi_k \Delta \theta_l \Delta E_m. \quad (4.10)$$

The total escape rate Q_{O^+} is then calculated by integrating over an area in the magnetotail over which the escape occurs. This area is assumed to be the size of the magnetotail, which is approximately $1.2 R_V$ in radius. As most measurements in the magnetotail are made at $X_{VSO} \approx -2 R_V$ the flux is averaged over $X_{VSO} = [-2.3, -1.4] R_V$, in order to account for statistical variations. The escape rate is then calculated as

$$Q_{O^+} = \sum_i \frac{1}{N_i} \sum_j F_x(X_i, R_j) 2\pi R_j \Delta R, \quad (4.11)$$

where N_i are the number of bins in X_{VSO} -direction, R_j is the mid-point of the radial bin and ΔR is the width in radial distance of each bin used.

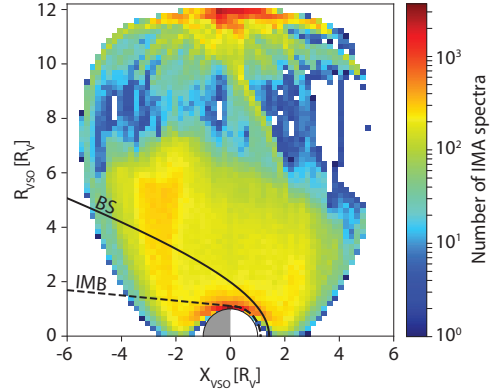


Figure 4.6: Number of IMA spectra measured in the Venusan plasma environment, shown in the VSO cylindrical coordinate system.

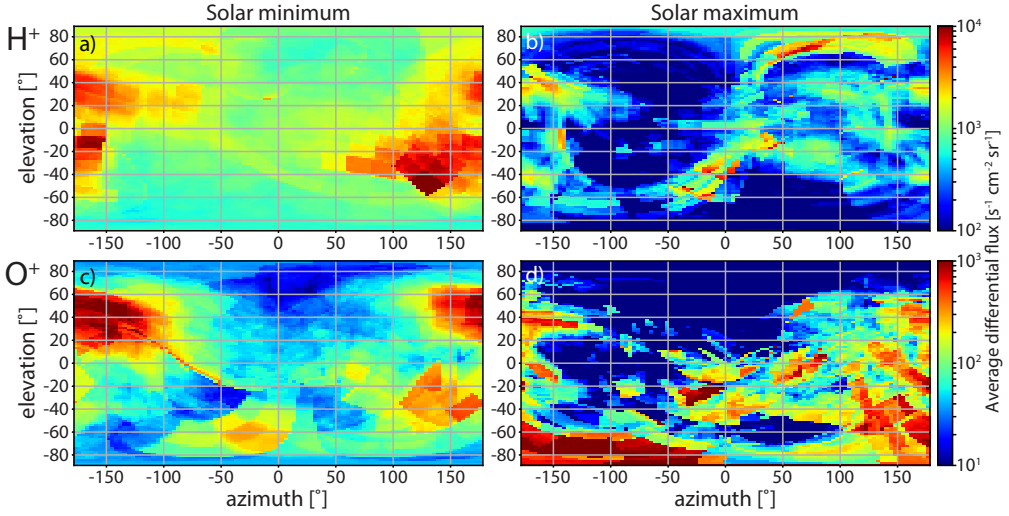


Figure 4.7: Examples of average ion distributions in the Venusian magnetotail (from Persson et al., 2018, paper I).

4.4.3 Calculating the Standard Error on the Escape Rates

To estimate the error on the escape rates, we use the standard error. The standard error gives an uncertainty of the mean for the calculated escape rate, and is here calculated through the bootstrap method (e.g. Efron and Tibshirani, 1994).

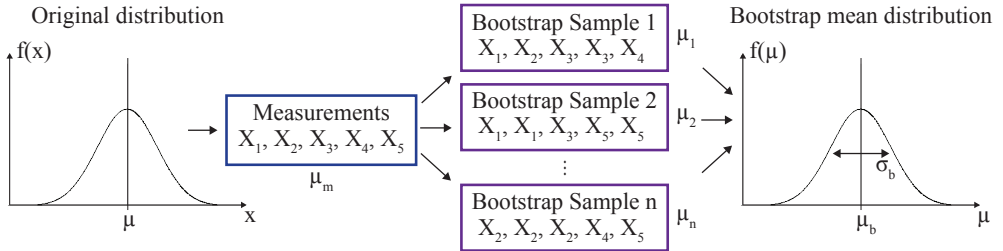
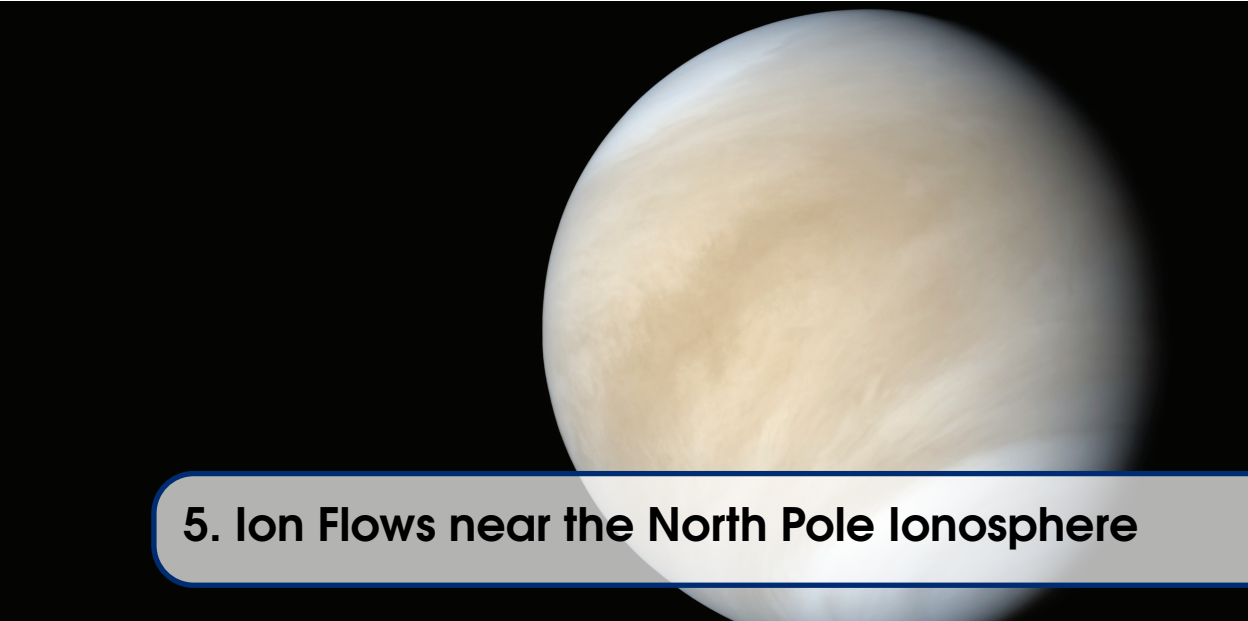


Figure 4.8: Example schematic of the bootstrap method using five measurements.

A simple example schematic of the bootstrap method is shown in Figure 4.8. In this case, if we have five measurements from the original distribution, with an average μ , we can extract the average of the measured samples μ_m and assume that $\mu = \mu_m$. However, μ_m has an uncertainty, a standard error, of σ . By sampling the measurements, with replacement, we get n number of new samples, each with a mean $\mu_1, \mu_2, \dots, \mu_n$. The means form a new distribution $f(\mu)$, which has been shown to form a normal distribution if n is large, from which we can

find a mean μ_b and a standard deviation σ_b . The standard deviation σ_b of the bootstrap mean distribution gives the estimate of the standard error. In this thesis μ_m is used as the average escape rate, and σ_b is used as the standard error of the mean.



5. Ion Flows near the North Pole Ionosphere

As mentioned in chapter 2, the ions in the ionosphere was found to have a flow of $\sim 2\text{--}5$ km/s from day-to-night in the equatorial region, which is supplying the nightside ionosphere (Knudsen et al., 1980; Miller and Whitten, 1991). If this flow is uniform over the entire disk, the flow would provide up to $5 \cdot 10^{26}$ O^+/s to the nightside, that can maintain both the ionosphere and provide ions for escape through the magnetotail (Knudsen and Miller, 1992). The aerobraking campaign of Venus Express provided an excellent opportunity to investigate if the ion flows in the polar region show similar patterns as near the equator, down to 130 km altitude. Analysis of the ion measurements by the VEx/IMA instrument made in Persson et al. (2019, paper II) is summarised below.

5.1 General Flow Patterns

The flow near the North Pole ionosphere, measured by VEx/IMA during 1 June to 31 July 2014, is shown in Figure 5.1, together with the flow patterns near the equator, measured by PVO (Miller & Whitten, 1991). It is clear that the flow pattern near the pole is not following the expected general trend of day-to-night. Instead the flow has a large dusk-to-dawn flow component, along the terminator. The dusk-to-dawn flow is interpreted as a consequence of a thermal pressure gradient along the terminator, forcing the ions to flow towards the polar region, in addition to the thermal pressure gradient along the day-night line (Persson et al., 2019, paper II). Investigation of the magnetic fields present in the measured region show that the ionosphere was mostly unmagnetised, with an ionopause altitude mostly located above 400 km, which indicates that the magnetic fields had little control of the ion flows. In addition, as the ion flow is preserved to very low altitudes, inside the collisional region, it is not likely to be significantly affected by a transfer of momentum from the solar wind.

The momentum transfer presumably has a larger effect at higher altitudes, as described in Lundin et al. (2011, 2014).

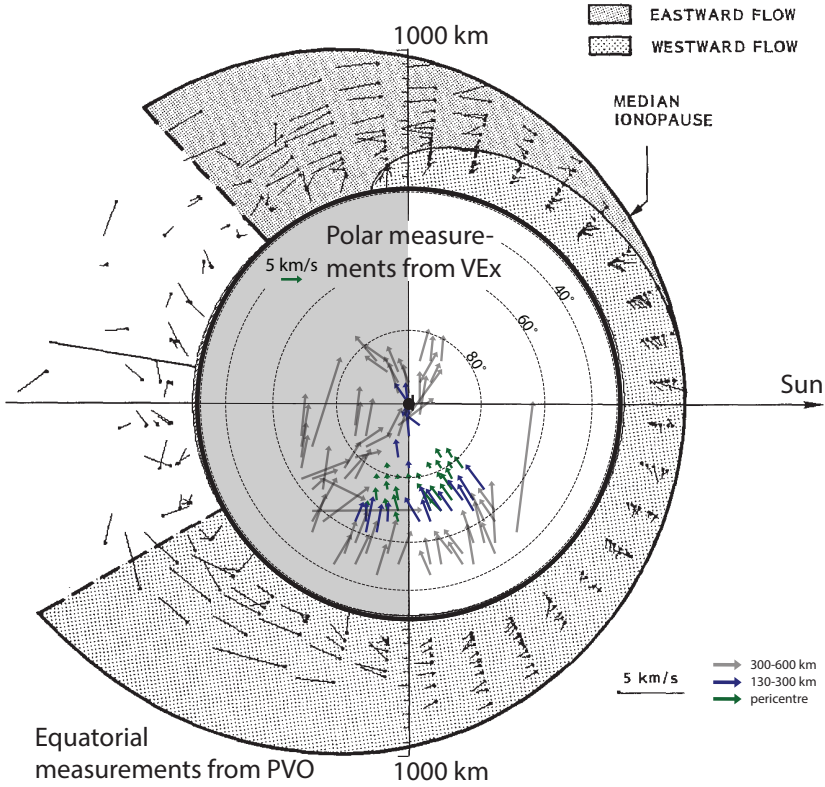


Figure 5.1: Flow vectors of heavy ions in the Venusian upper ionosphere. The polar measurements in the centre of the disk (North Pole) is made by VEx/IMA (Persson et al., 2019, paper II), while the equatorial measurements outside the disk edge (equator) is made by PVO (Adapted from Miller and Whitten, 1991).

5.2 Altitude Profiles

The altitude profile of the density and vertical velocity of the ions measured by IMA is shown in Figure 5.2. The density profile shows a clear trend of decreasing with increasing altitude, with a scale height of 15 km below 180 km altitude and 200 km above 180 km altitude. This agrees with measurements and models of the Venusian ionosphere (Fox and Sung, 2001; Taylor et al., 1980), assuming the dominant species as O^+ above an altitude of 180 km and O_2^+ below (compared with Figure 2.1b). The measured absolute density is lower

than the expected, which is a consequence of that the IMA instrument was not designed to make measurements near the ionospheric peak of Venus. Therefore, the absolute density data should be interpreted with significant care. Instead, the relative density and its variations with altitude is investigated. The shift in scale height of the ions near 150 km indicates a shift in the major species, as we move from a region dominated by photochemistry, to the diffusion region above (Fox and Sung, 2001).

Furthermore, the vertical velocity altitude profile shows that the ions are dominantly moving downward below 400 km altitude, while a larger spread is apparent above 400 km altitude. This indicates that the ions are collisionally coupled with the neutral atmosphere below 400 km altitude, while above 400 km altitude the ions are coupled with the solar wind (Lundin et al., 2011, 2014).

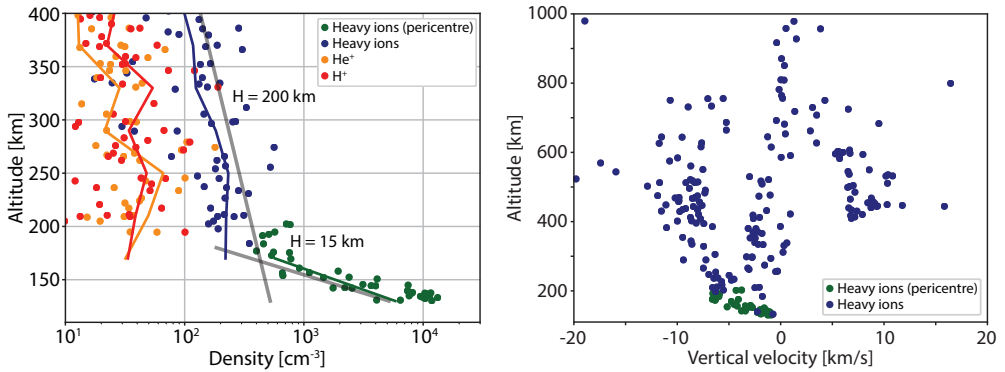


Figure 5.2: Altitude profile of a) density (Persson et al., 2019, paper II) and b) vertical velocity (upwards is positive), measured by Venus Express during 1 June to 31 July 2014.

5.3 Coupling with Neutrals and Effect on Escape Rates

The flow of ions from dayside to nightside is important for both the maintenance of the nightside ionosphere and the escape of ions to space. As mentioned earlier, if there was a uniform flux of ions such as that found near the equator, the total flow of ions would be $\sim 5 \cdot 10^{26} \text{ O}^+/\text{s}$ (Knudsen and Miller, 1992). However, as the flow is found to not be uniform over the entire disk, the total flux of ions is presumably less. Yet, considering that the total flux is one to two orders of magnitude larger than the escaping flux of around $(3 - 6) \cdot 10^{24} \text{ O}^+/\text{s}$ (Futaana et al., 2017), the ionospheric flows is not considered to severely limit the escape rates. Compare with Mars, where it was found that the flux from dayside to nightside potentially limits the total escape of ions (e.g. Ramstad et al., 2017). Further measurements are needed in order to understand the full flow pattern over the entire disk of Venus and its potential effect on the escape

of atmospheric constituents. Details on the measurements needed to address this question are laid out in subsection 7.4.2.

In addition, the flux of ions found in this study shows that there is a fast flow of ions deep into the collisional part of the atmosphere, down to 130 km. The fast flow is also shown to have a clear downward component at the lowest altitudes. In this region, the ions should be collisionally coupled with the neutral atmosphere. This indicates that a loss of momentum from the ions to the neutrals should exist, which was also shown through the loss of mass flux of the ions with decreasing altitude (Lundin et al., 2011). However, it is still not fully clear how the thermosphere, ionosphere and solar wind are coupled, and only more measurements can answer this question. Potential new measurements that can address this question are suggested in subsection 7.4.2.



6. Ion Escape Through the Magnetotail

Today, the net escape through the magnetotail is the most important channel for escape of atmospheric constituents from Venus (chapter 3). In this chapter, the results of the studies on the average ion escape rates in the magnetotail are summarised. The escape rates are determined for different constrained parameters, e.g. solar activity and solar wind energy flux in order to evaluate the dependence between the parameter and the escape rate. These escape rates were calculated through average distributions, which are used to calculate the total integrated flux over the magnetotail. The method is described in section 4.4.

6.1 H^+ and O^+ Ion Escape Over the Solar Cycle

The escape of both H^+ (Q_{H^+}) and O^+ (Q_{O^+}) is important for the atmospheric evolution of Venus. The early data from VEx/IMA showed that the ratio of escape rates between H^+ and O^+ is 1.9, i.e. approximately the stoichiometric ratio of water (Fedorov et al., 2011). We extended the investigation to over almost a full solar cycle and divided it into two parts: 2006-2009 (solar minimum) and 2010-2014 (solar maximum). We found that the escape rate ratio changes from approximately 2.6 to 1.1 from solar minimum to solar maximum. The escape rates are summarised in Table 6.1. This change mainly comes from the change in H^+ escape rates, attributed to a significant increase in Venusward flows (see section 6.2) from solar minimum to solar maximum. A summary of all H^+ to O^+ escape rate ratio studies is shown in Figure 6.1.

6.2 Return Flows in the Magnetotail

One interesting feature in the magnetotail of Venus is the return flows, i.e. ions that flow back towards Venus far out in the magnetotail. These return

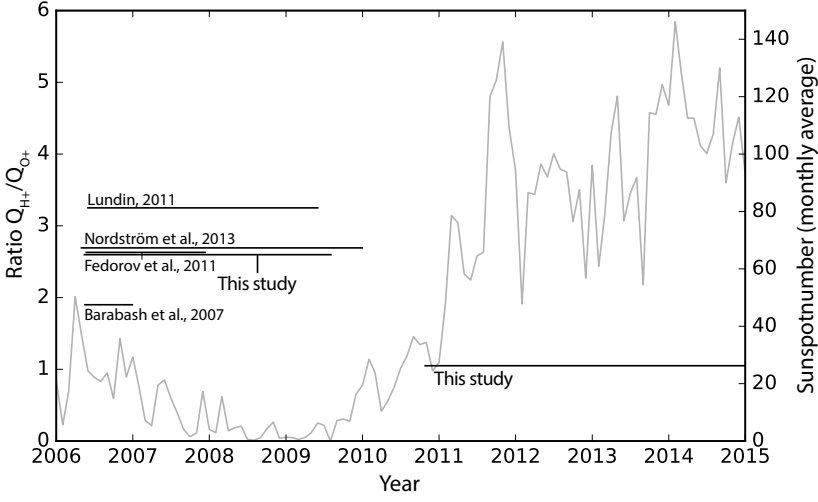


Figure 6.1: The ratio of the H^+ to O^+ escape rates in the Venusian magnetotail from different time periods. The grey line show the monthly average sunspot number (from Persson et al., 2018, paper I).

Table 6.1: Average escape rates with the standard errors for H^+ and O^+ and corresponding escape rate ratio calculated for solar minimum (2006-2009) and solar maximum (2010-2014) (from Persson et al., 2018, paper I).

	Solar minimum (2006-2009)	Solar maximum (2010-2014)
H^+ escape rate Q_{H^+} , s^{-1}	$(7.6 \pm 2.9) \cdot 10^{24}$	$(2.1 \pm 1.2) \cdot 10^{24}$
O^+ escape rate Q_{O^+} , s^{-1}	$(2.9 \pm 1.1) \cdot 10^{24}$	$(2.0 \pm 1.1) \cdot 10^{24}$
Escape rate ratio, Q_{H^+}/Q_{O^+}	2.6	1.1

flows seem to increase from solar minimum to solar maximum, which lead to a large decrease in the total net escape rate at solar maximum, specifically for protons (Persson et al., 2018, paper I). Examples of the flux maps for solar minimum and maximum, for H^+ and O^+ , at Venus is shown in Figure 6.2, where it is clearly seen that the return flows increase during solar maximum, most strikingly for protons.

More details of the return flows can be found by investigating the velocity distribution function of O^+ in the Venusian magnetotail. An example is shown in Figure 6.3. Here, the average distribution of the O^+ is made over the magnetotail, using a slice in the X_{VSO} direction at -2.3 to -2.0 R_V , separated by location with respect to the solar wind motional electric field \vec{E} . The $+\vec{E}$ quadrant is

defined as measurements made within $\pm 45^\circ$ from $+\vec{E}$, and the $-\vec{E}$ quadrant is defined as measurements made within $\pm 45^\circ$ from $-\vec{E}$ direction (Persson et al., 2020c, paper V). The distributions show that there is a clear difference between the location, where in the $+\vec{E}$ quadrant the ions have a larger density of high tailward velocity, while in the $-\vec{E}$ quadrant the ions have a larger density of high Venusward velocity. This indicates that there is a difference in the mechanisms that accelerate the ions in the different regions in the Venusian magnetotail, structured by the upstream solar wind and IMF directions. In the $+\vec{E}$ quadrant, the ions are accelerated tailward by the $\vec{j} \times \vec{B}$ force (the 2nd term in Equation 2.2), created by the draping pattern of the IMF in the magnetotail. In the $-\vec{E}$ quadrant the IMF draping pattern is more complex (Rong et al., 2014; Zhang et al., 2010), which can cause a $\vec{j} \times \vec{B}$ force directed towards Venus in some cases (Masunaga et al., 2019). Another suggested cause is magnetic reconnection (Kollmann et al., 2016), where the results here suggest that reconnection, if it is the cause, should be occurring at a higher frequency in the $-\vec{E}$ hemisphere (Persson et al., 2020c, paper V).

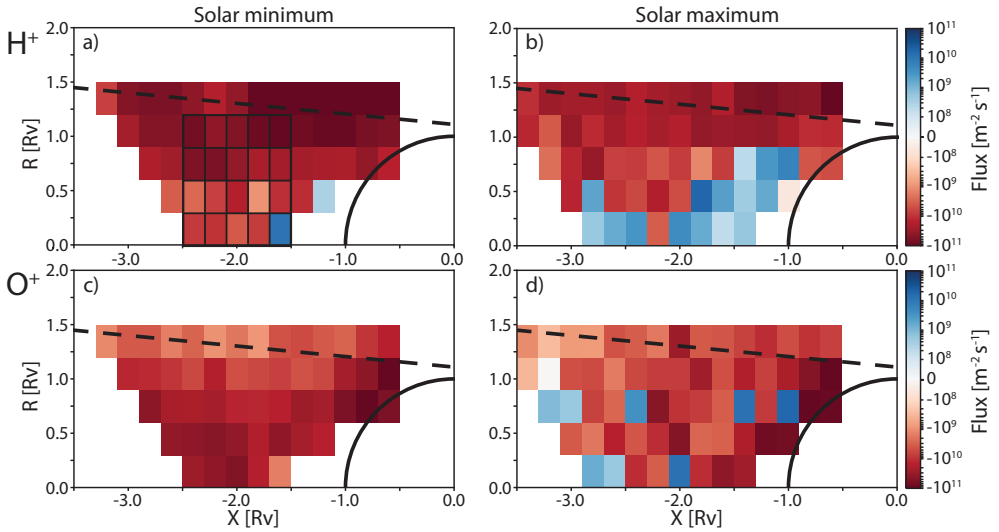


Figure 6.2: Maps of average fluxes in the Venusian magnetotail for H^+ and O^+ , during solar maximum and minimum. The reddish bins show fluxes in the anti-sunward direction, and the bluish bins show fluxes in the Venusward direction. The black boxes in a) show the volume used in the escape rate calculations (from Persson et al., 2018, paper I). The black circle indicate the Venusian surface, and the dashed line is the theoretical position of the IMB (Martinez et al., 2008).

A comparison of the H^+ and O^+ bulk flows adds additional information about the nature of the return flows. Sometimes, when bulk flow of protons are

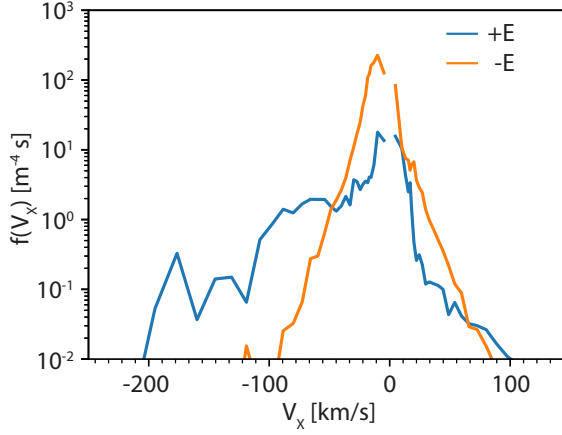


Figure 6.3: The average velocity distribution function in the Venusian magnetotail. The data is separated into a $+\vec{E}$ and $-\vec{E}$ quadrant, with an average over $X_{VSO} = [-2.3, -2.0]$, $R_{VSO} < 0.9 R_V$ (from Persson et al., 2020c, paper V).

directed towards Venus, the bulk flow of heavy ions is simultaneously pointed tailward (Kollmann et al., 2016). This indicates that the mechanisms for the return flows are dependent on mass. This also suggests that the mechanism that produces the return flows is magnetic reconnection. VEx has seen signatures of reconnection in the magnetic field and plasma data at Venus (Zhang et al., 2012) and reconnection has been sighted several times at Mars (Harada et al., 2015, 2017). As Mars can be said to have a hybrid magnetosphere, where the induced magnetic fields interact with the localised crustal magnetic fields on the Martian surface which create a different magnetic topology in the near-Martian magnetotail compared to Venus, the reconnection signatures at Mars may come from reconnection between the crustal fields and the IMF (e.g. Luhmann et al., 2015). Clear statistical evidence for reconnection in the Venusian magnetotail is still not found.

In order to fully understand the mechanisms responsible for the significant return flows at Venus, both more measurements and modelling efforts are needed, together with comparisons of measurements and modelling results. In addition, a more detailed comparison between Venus and Mars magnetotails would be very valuable. As there are both similarities and differences between the Venusian and Martian magnetotails, e.g. size, escape velocity, magnetic fields and interaction with the solar wind, a comparison between them could provide more information on the physical processes responsible for the return flows at both planets.

6.3 O⁺ Ion Escape Dependence on Upstream Parameters

By separating the measurements of O⁺ fluxes in the magnetotail into ten bins of upstream conditions, a more detailed picture, than from the solar minimum and maximum results, was realised. The upstream solar wind energy flux was divided into five bins, which each was divided into a high and low solar EUV radiation flux case. For each of the ten conditions the total escape rates of O⁺ were calculated, which are shown in Figure 6.4a. The division shows that the escape rates at present day is positively correlated with the energy available in the upstream solar wind, but not clearly dependent on the solar EUV flux. In other words, the ion escape from Venus is dependent on the amount of energy and momentum transferred from the solar wind to the Venusian ionospheric particles. This indicates that Venus is energy-limited, i.e. that the amount of energy transferred to the Venusian particles is limiting the total escape rates (Persson et al., 2020a, paper III).

In addition to the VEx/IMA measurements, the escape rate results from the PVO mission is summarised in Figure 6.4a. It is clear that the upstream solar wind energy flux was generally higher during the PVO mission, which presumably is the reason for the increased escape rates during that time. There is a general agreement between the VEx and PVO measurements, two completely different missions with different instruments, as the PVO results fall within a factor of 2-3 from the fitted trend to the VEx/IMA escape rate measurements.

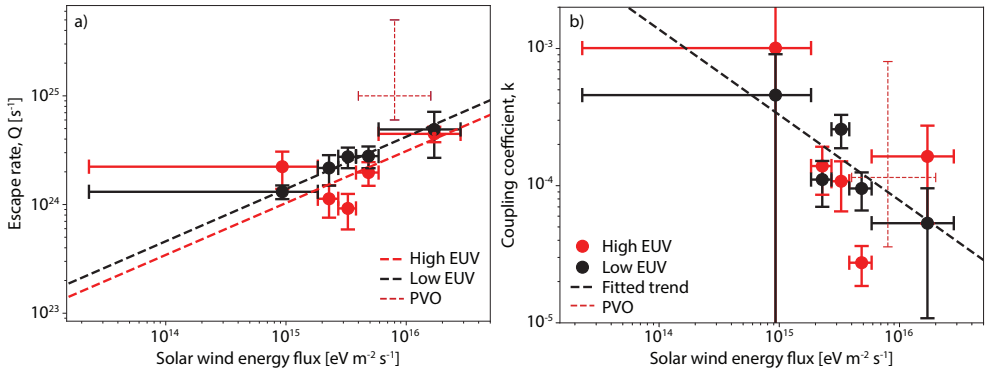


Figure 6.4: The dependence on the solar wind energy flux for a) the O⁺ escape rate and b) the coupling coefficient, measured by VEx/IMA during 2006-2014 (from Persson et al., 2020a, 2020b, paper III & IV).

6.4 Coupling Between Solar Wind and Escaping Ions

An important question raised from the dependence between the escape rates and the available upstream solar wind energy, is how efficient the energy transfer

is. The efficiency can be investigated from a constructed coupling coefficient k , defined as the ratio between the power escaping from Venus in the form of ion escape P_Q and the available solar wind power P_{sw}

$$k = \frac{P_Q}{P_{sw}} = \frac{\sum Q_{O^+}(E) \cdot E}{F_{sw,E} \cdot A}, \quad (6.1)$$

where E is the energy, $F_{sw,E}$ is the solar wind energy flux, A is the area over which the energy is transferred to the ionospheric particles, and $Q_{O^+}(E)$ is the escape rate energy dependence. Figure 6.4b show the coupling coefficient plotted against the upstream solar wind energy flux. The results indicate that the energy transfer is very inefficient, with an average coupling of 10^{-4} , i.e. only 0.01 % of the total available solar wind energy is transferred to the net escaping ions. In addition, the coupling decreases as more energy is available in the upstream solar wind (Persson et al., 2020b, paper IV).

6.5 Extrapolating the Escape Rates to 3.9 Ga

The relation between the O^+ escape rate and the upstream solar wind energy flux can be used to extrapolate the escape rates backwards in time until 3.9 billion years ago (Ga). By estimating the evolution of the solar wind through observing neighbouring Sun-type stars (Airapetian and Usmanov, 2016; Wood, 2006), the escape rate evolution is found and presented in Figure 6.5. The total accumulated escaping mass of O^+ ions from Venus is $3.2 \cdot 10^{16}$ kg, if the escape in the magnetosheath is included (~ 30 % of the total O^+ ion escape; Masunaga et al., 2019).

Assuming that all the escaping O^+ ions comes from water, which is appropriate as the ratio between the H^+ and O^+ escape rates is so close to the stoichiometric ratio of water, the total mass of water would be $3.6 \cdot 10^{16}$ kg. This mass corresponds to approximately 0.02-0.6 m of water, if spread equally over the entire surface of Venus. The historical water content of Venus is assumed to be in the range between 4-525 m (Way et al., 2016). Therefore, the simple extrapolation of current states imply that the non-thermal escape of O^+ ions over the past 3.9 Ga cannot account for the total loss of water from Venus.

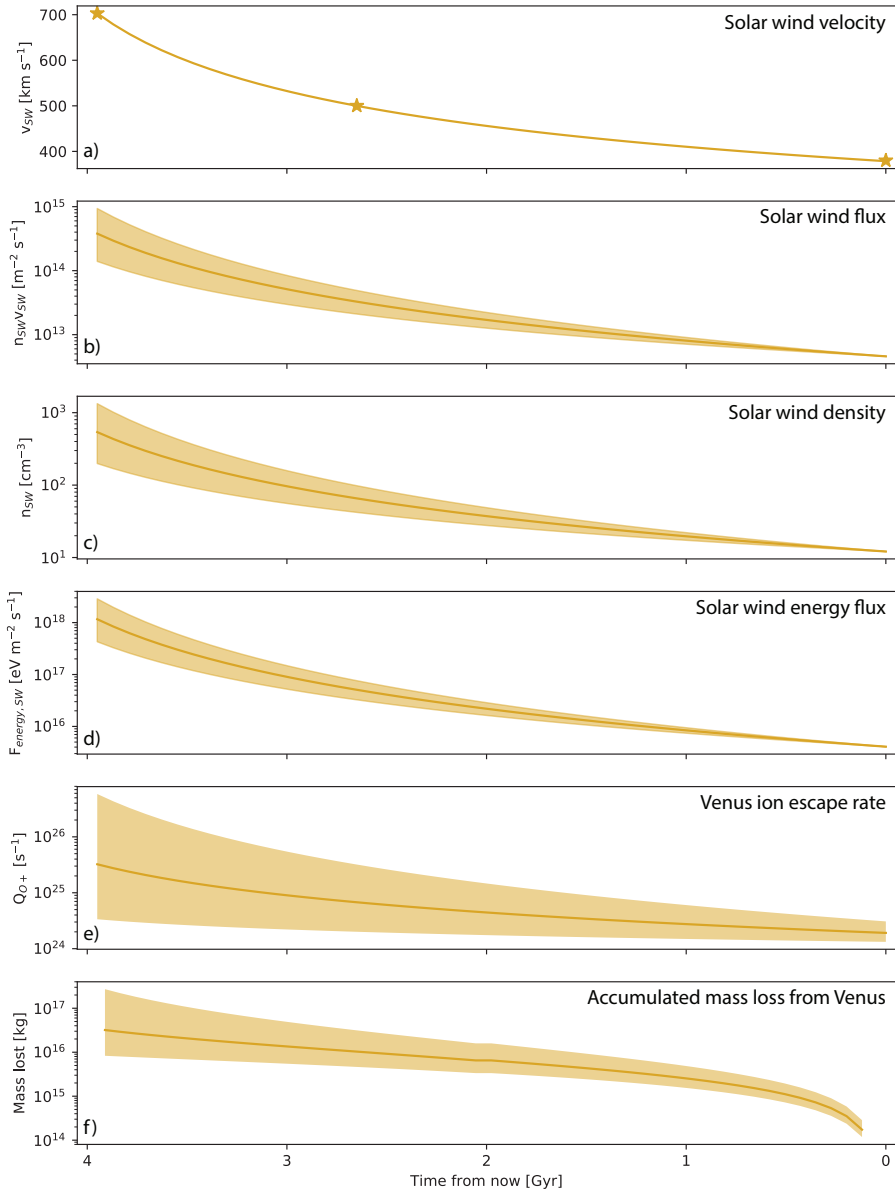
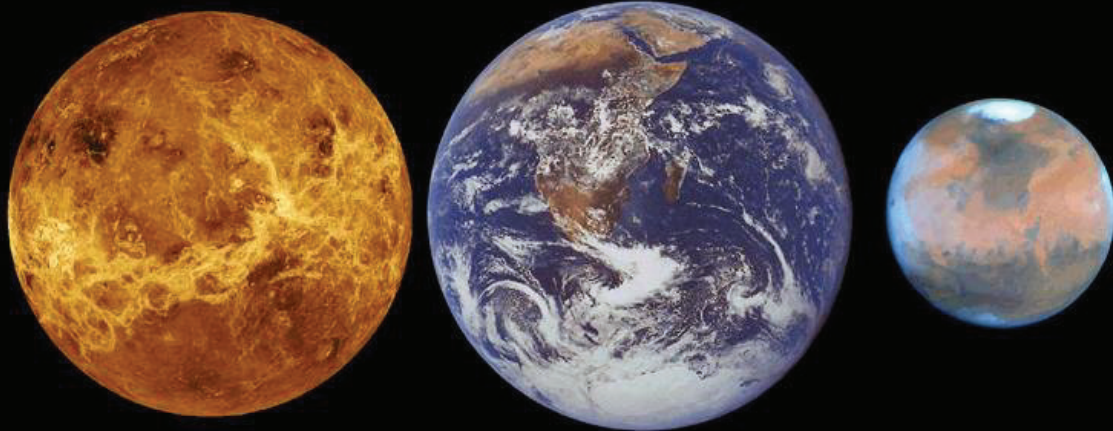


Figure 6.5: Extrapolation from now to 3.9 Ga of the upstream solar wind parameters and the escape rates from Venus, using the relation between solar wind energy flux and O^+ escape rates (from Persson et al., 2020a, paper III).



7. Conclusions and Implications

“Observation: there was absolutely nothing to see on Venus. Conclusion: it must be covered with life.”

– Carl Sagan, *Cosmos*

In this thesis the interaction between the solar wind and the Venusian atmosphere was investigated, with a focus on the escape of O^+ and H^+ ions that results from this interaction. The O^+ escape rates from Venus was found to increase with an increase in energy present in the upstream solar wind. However, the percentage of energy transferred from the solar wind to the atmospheric particles decreases as the solar wind energy flux increases. This indicates that the Venusian atmosphere is efficiently preventing the solar wind from stripping the atmosphere of its constituents. Extrapolating the simple relation between the solar wind and the escape rates to 3.9 Ga, together with the evolution of the solar wind, the total escape in the form of ions was calculated to be on the order of 0.02-0.6 m of water, if spread equally over the Venusian surface. In other words, the main results found in this thesis indicate that the escape processes for oxygen, presently operating at Venus, cannot explain the loss of an ocean of water from the surface of Venus. In this chapter, the results are put in perspective of the other terrestrial planets in our solar system (section 7.1) and the historical presence of water (section 7.2) and potential life (section 7.3) on Venus. In the end, future measurements needed to provide further understanding of the results of this thesis are discussed, together with a summary of the potential future missions that are planned for Venus.

7.1 Venus, Earth and Mars

By comparing the escape rates at Venus with those at Mars and Earth, we can investigate how the escape rates depend on the planetary characteristics. The O^+ escape rates at Mars was recently found to be highly dependent on the solar EUV radiation flux, but not as dependent on the upstream solar wind dynamic pressure (Ramstad et al., 2015). Due to the low gravity of Mars the escape energy for O^+ is only ~ 2 eV, which means that many of the ions near the exobase will reach above the escape energy and be able to leave the planet without the need of additional energy input from the solar wind. Instead, the limitation of the escape rates comes from the amount of ions that are produced and transported to the upper ionosphere where it can escape. This is an important difference between Venus and Mars, that leads to a difference in their escape rates. However, both for Venus and Mars, the coupling between the upstream solar wind power and the escaping power decreases as the available energy in the solar wind increases (paper IV: Persson et al., 2020b; Ramstad et al., 2017). In addition, extrapolation of the escape rates to 3.9 Ga at both Venus and Mars gives very low total escape, incapable of explaining the atmospheric evolution at neither of the planets (Persson et al., 2020a; Ramstad et al., 2018, paper III).

In addition to comparing the O^+ escapes at Venus and Mars with each other, it is interesting to compare the H^+ escape from Venus with the O^+ escape from Mars. The escape energy for H^+ at Venus is ~ 0.5 eV, while the escape energy for O^+ at Mars is ~ 2 eV. The low escape energies mean that the ions don't need a significant acceleration in order to reach above escape energy, as stated above. Our preliminary results of the H^+ escape and its dependence on upstream parameters at Venus indicate that the H^+ escape is less dependent on the upstream solar wind energy than the O^+ escape at Venus. The escape shows tendencies of decreasing with an increase in the upstream solar wind energy flux, which is similar to results of O^+ escape at Mars (Ramstad et al., 2015). However, the H^+ is highly affected by return flows in the magnetotail (Persson et al., 2018), and the separation between planetary and solar wind H^+ , which is currently being evaluated. The final results of the continued H^+ escape study will be interesting both for further comparisons with the Martian O^+ escape, and for the evaluation of the water escape from Venus.

Earth, on the other hand, has almost the same escape velocity as Venus, but has a completely different interaction with the solar wind. Earth has a strong intrinsic magnetic field, which interacts with the solar wind and creates a magnetosphere with a radius almost 10 times larger than the Venusian induced magnetosphere. The escape of O^+ at Earth increases with an increase in the solar wind dynamic pressure, while it does not change significantly with changes in the solar EUV flux (Schillings et al., 2019). This is very similar to the O^+ escape at Venus and indicates that the important factor for the escape rate might rather be gravity, not the type of interaction with the solar wind. Although, in contrast with both Mars and Venus, the coupling between the escape from Earth and the available energy upstream of the magnetosphere increases with

increasing power in the upstream solar wind, especially after a threshold in the available energy is reached. This instead indicates that the interaction with the solar wind actually funnels energy from the solar wind to the atmospheric particles, which lead to a higher escape of atmospheric particles. Currently, there is a lot of interest in understanding the difference between the escape rates at Venus, Earth and Mars. The aim is to understand if the intrinsic magnetic field at Earth really protects Earth's atmosphere or not, which recent escape rate studies indicates is not true, and if the knowledge can be transferred to exoplanets. If we can understand the interaction of the exoplanets and their stellar winds, and how this interaction affect their atmospheric evolution, it could be possible to infer more on the past, present and future habitability of the studied exoplanets.

7.2 Water on Venus

The extrapolated O^+ escape rates, made in this thesis (chapter 6), indicates that the loss of water through ion escape to space cannot explain the loss of an Earth-like water ocean present on Venus 4 billion years ago. This leads us to the question on if there ever was as much water on Venus, and if so, where did all the water go? In principle, there are two directions the water can escape through, either through escape to space, or diffusion into surface materials. The current escape rates are very low, but in the early Venusian history the thermal and hydrodynamical escape was strong enough to pull out a significant amount of hydrogen, and some of the oxygen, which was originally part of water (Kasting and Pollack, 1983). There are also indications that a significant amount of the remaining oxygen has reacted with the surface materials of Venus and gone into the ground or into the mantle of Venus (e.g. Albarède, 2009). However, an atmosphere with such a high surface pressure as Venus may have a very low diffusion rate into the surface, preventing the loss of the remaining oxygen from the atmosphere (Gillmann and Tackley, 2014). If the oxygen did oxidise the crust, it would result in an oxidised rock layer of around 50 km thick (Lécuyer et al., 2000).

The assumptions of a large water content of the Venusian atmosphere comes from measurements of a high D/H ratio, 150 ± 30 times that of Earth's (Donahue et al., 1997; Donahue and Hartle, 1992), which indicates a fractionated long-term escape. However, the observed high D/H ratio may be explained, at least partly, by a large comet impact that brought water of a high D/H ratio, or by catastrophic resurfacing events and accompanied outgassing within the past 1 billion years (Grinspoon, 1993; Taylor and Grinspoon, 2009).

Distinguishing between these conflicting hypotheses about the history of water in the Venusian atmosphere is challenging (see larger discussion of the hypotheses in Way and Del Genio, 2020). The results of this thesis suggest that water either escaped in its early history, diffused into the surface, or that Venus did not have as much water as suggested. Further studies using both available

and new measurements, with modelling efforts, will provide more information to constrain the Venusian atmospheric water history.

7.3 Life on Venus

7.3.1 Past

Considering that Venus once might have had a significant amount of water in either its atmosphere or as liquid on the surface, it is tempting to think that Venus once hosted life, or was habitable. Venus lies at the edge of the habitable zone (HZ), and inside the extended HZ. Mars has been included in the zone, as it seems likely that it hosted life at one point, while Venus is still under debate whether it ever hosted life (Merino et al., 2019; Rothschild, 2007). One interesting part is therefore to use Venus in the context of exoplanets. Assuming Venus as an exoplanet, we can make experiments, and analogies on Venus, in order to learn more on exoplanets and their potential habitability.

7.3.2 Present

Venus today very much resembles the place we would call hell, with extreme temperatures, high pressures and strong winds. However, does that mean that there is no life on Venus? Recent findings by Greaves et al. (2020) show that there exist large amounts of phosphine in the cloud layer of Venus, with a higher content than exist on Earth. The creation of such large amounts of phosphine on Venus cannot be explained by neither any known chemical reactions, nor by volcanic outgassing or the influx of meteors (Bains et al., 2020). It is known that anaerobic extremophiles, or microbes, on Earth can create phosphine. Therefore, the results suggest there could be microbes in the cloud layer that is creating the phosphine that was observed, but it could also be created by some chemical reactions that are still unknown (Greaves et al., 2020). The potential microbes are hypothesised to have a life cycle that is partly present in the sulphuric acid droplets in the clouds (Limaye et al., 2018; Seager et al., 2020). As there are life that can exist in the most inhospitable places on Earth, such as in hypersaline lakes and acid mine drainages (Merino et al., 2019; Rothschild, 2007), it is suggested that life on Venus could also manage to survive the very acid cloud droplets (Schulze-Makuch et al., 2004). However, there are still many obstacles that the potential life in the Venusian clouds have to overcome, such as not drying out in the very dry atmosphere, and managing the sulphuric acid, which concentration causes it to be $\sim 10^{11}$ times more acidic than the most acid lakes with life on Earth (Seager et al., 2020). Nevertheless, the phosphine findings are very exciting, and more investigations and measurements are needed in order to further understand these results and its potential indication of life on Venus. There are already several proposed future missions to Venus which could provide the necessary measurements. These missions are summarised in subsection 7.4.4. In addition, hopefully, the phosphine findings will cause more missions to Venus to be proposed in the future.

7.3.3 The future is ♀?

There is a lot of interest in sending humans to Mars, but what about Venus? There are some studies suggesting that humans can be sent to Venus, and that it could even be easier than sending them to Mars (e.g. Arney and Jones, 2015). Let's consider the differences between Mars and Venus. Venus is closer to the Sun than Mars, meaning that we need smaller solar panels to receive the same power output. The travel time to reach Venus is only around 100 days, which is significantly shorter than reaching Mars. Venus has a thicker atmosphere than Mars, and humans in the atmosphere would be more protected on Venus than on Mars from bursts of radiation in the form of e.g. energetic particles, which deposit their energy at altitudes above the cloud tops (Nordheim et al., 2015). The Venusian gravity is very close to Earth's, where the much lower gravity on Mars is a problem for any humans present due to bone degradation. On the other hand, the most important issue about Venus is that the surface is anything but hospitable for humans. This is solved by using balloons, or Zeppelins, floating at around 60 km altitude, which is a mission concept currently in development (HAVOC, Arney and Jones, 2015), see Figure 7.1. The clouds are of course composed of sulphuric acid, which destroys most materials, and will be a challenge to overcome. However, the clouds also has a very large albedo, meaning that we can have solar panels both above (pointing at the Sun) and below (pointing at the clouds). Indeed, the cloud cover also travels with a high speed, so any aircraft would move around Venus in about 4 days, which is better than the over 100 day long nights on the surface. Perhaps sending humans to Venus is not the first priority at the moment, but the idea should definitely not be removed from our minds too quickly just because Venus might seem like the actualisation of the human hell.

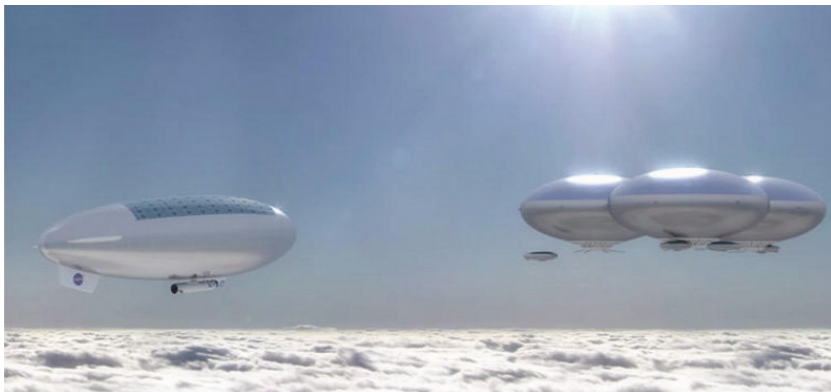


Figure 7.1: An artist's visualisation of the HAVOC mission concept, where Zeppelins would carry humans in the cloud tops of Venus (e.g. Arney and Jones, 2015). Courtesy of NASA.

7.4 Desired New Measurements in the Future

Even though Venus has been studied extensively, through many spacecraft missions and with modelling, there is still a lot more to be learnt. From the conclusions of this thesis, several suggestions can be made on potential future projects, which would help to further improve our understanding of the Venus-solar wind interaction and its effect on the atmospheric evolution. Here a summary of three such suggestions is made.

7.4.1 Space Weather Events

Analysing a massive space weather event at Venus would help understanding how the upper range of the upstream solar wind parameters, and the Solar Energetic Particles (SEPs), affect the escape rates. It is clear that an increase in solar wind dynamic pressure, or energy flux, causes an increase in the escape rates of heavy ions (Dimmock et al., 2018; Edberg et al., 2011; Persson et al., 2020a, paper III), and that SEPs, with their MeV energies, can penetrate into the ionosphere and cause significant additional ionisation (Nordheim et al., 2015). In the studies of this thesis the Venusian plasma environment is assumed to react systematically to each range of upstream parameters. However, during extreme space weather events the atmospheric response may be non-linear. Only more measurements can provide additional information on the effect from extreme space weather events.

The results from the measurements depend highly on where in the plasma environment the measurements are made. For example, the space weather events can significantly increase the rate of pickup ion escape from Venus (Luhmann et al., 2006; McEnulty et al., 2010), but this is only visible in spacecraft measurements if the spacecraft passes through the “plume” at the right moment during the space weather event. If the spacecraft misses the plume, the net escape rates might be underestimated. Likewise, it is challenging to get the global picture from a single point measurement during a space weather event that usually only lasts for a few hours when, for example, the orbital period for VEx is 24 hours. Additionally, for the SEPs, a timed correlation between the impact of the SEPs and the effect on the ionosphere is needed, in order to separate them from the effects of other parts of the space weather event.

In Figure 7.2 an example of a space weather event measured by VEx is shown. Here we can clearly see several parts of an ICME hitting Venus. First, the SEPs arrive at Venus on Nov 3 (1.), which was emitted by the Sun at the time of the CME occurring in the solar surface. These travel at high speeds, along the magnetic field lines, and can therefore arrive at Venus several days beforehand (Reames, 1999). This provides ample time for the Venusian plasma environment to react. Unfortunately, VEx did not provide low altitude measurements during this time. On Nov 5, the ICME shock front (2.) reaches Venus, and the SEPs accelerated by the shock front (Reames, 1999) are clearly seen in the IMA background data (3.), i.e. measured penetrating particles in the instrument. The magnetic fields show the typical magnetic field rotation

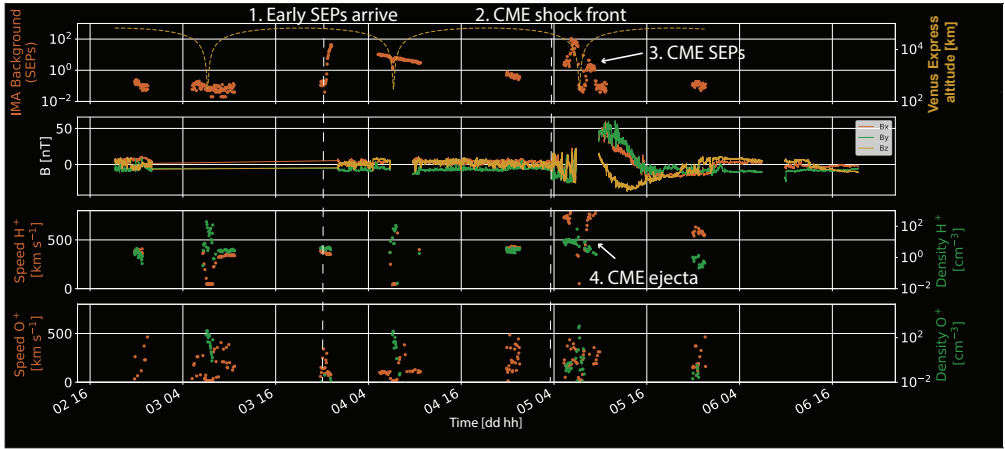


Figure 7.2: Example of a solar event at Venus in November 2011, measured by VEx. a) background counts of IMA from penetrating high energy particles, such as SEPs, measured in a part of the instrument MCPs which should not be reached by real ion measurements. b) Magnetic field measured by MAG. c) Speed and density of protons (mainly solar wind origin) measured by IMA and d) speed and density of heavy ions (O^+ , planetary origin) measured by IMA (presented by Persson et al. at EPSC 2019).

signature of an ICME ejecta cloud as it passes Venus (4.). The solar wind measurements show a clear increase in proton velocity as the ICME travels past Venus at a very high speed. There are also evidence for an increase in the planetary heavy ion density, which indicates an increase in escape rates as a result of the ICME. Dimmock et al. (2018) showed with a hybrid simulation, where electrons are treated as a fluid and ions as kinetic particles, that the escape during this event increased by $\sim 30\%$. However, even though it is already known that the ICME itself causes large disturbances in the Venusian plasma environment (e.g. Futaana et al., 2008; Xu et al., 2019), it is still unclear exactly how much and how the SEPs play a role in this.

Multipoint measurements would be able to provide a more global picture during such space weather events. A timed connection between the upstream parameters and the reaction of the Venusian plasma environment can be reached, and remove the need for assuming quasi-stable upstream parameters, which is used in this thesis. In addition, it could provide more details on the ionosphere-magnetosphere coupling during such an event.

7.4.2 Ionosphere-Thermosphere Coupling

There is still unanswered questions on the energisation of the ions in the ionosphere, and how the ionosphere and thermosphere couple (see chapter 5). Is there energy and momentum transfer between the neutrals and the ions near or

below the exobase? Does this lead to energy being transferred down to lower altitudes, or to energy being transferred from the neutrals to the ions that lead to ions reaching higher altitudes and escape? Only further measurements at Venus can help answer these questions. A mission with a plasma consortium providing measurements of low-to-medium energy and a high time resolution at lower altitudes would be excellent. As IMA on board VEx was not designed to make ionospheric measurements, the time resolution was not optimised for the ionosphere, as described in chapter 5. Therefore, a higher time resolution would be able to provide a more detailed altitude profile with the variations present inside the thermosphere/ionosphere. If measurements would be made in the southern hemisphere, near the pole, it would also help to further understand the flow patterns in both the thermosphere and ionosphere and how they couple: Does the dusk-to-dawn flow along the terminator (see chapter 5) prevail near the south pole, or is it flipped and have a pattern of dawn-to-dusk? These measurements would provide a great addition to really understanding the physical processes involved in the ion flows.

If the plasma measurements could also be coupled with measurements of the neutrals, we can further characterise the coupling between the neutrals and ions. For example, the MAVEN mission at Mars showed that the wave structure of the neutral atmosphere is connected with the wave structure of the ions (Mayyasi et al., 2019). Similar measurements at Venus would be of substantial interest for the understanding of the “first few eV” question; How are the ions first accelerated that lead them to reach the upper ionosphere, where they are further accelerated through the interaction between the solar wind and the Venusian atmosphere (the acceleration processes through the solar wind interaction is summarised in chapter 3)? For example, VEx torque measurements during the ADE campaigns show significant wave structures in the upper thermosphere (e.g. Müller-Wodarg et al., 2016; Persson, 2015). Whether these gravity wave structures also propagate to the ions is still an open question, which can only be answered with high time resolution measurements made simultaneously of neutrals and ions.

7.4.3 Sputtering

Sputtering is a largely unmeasured part of the atmospheric escape from Venus. As described in subsection 3.2.3, sputtering occurs when an ion or neutral particle is accelerated towards the atmosphere and collide with the atmospheric particles. The accelerated ion or neutral particle may transfer some of its energy to the atmospheric particle that can reach above escape energy and escape the atmosphere. There are some studies that show the potentially large contribution of sputtering to the escape rates of oxygen from Venus using modelling (e.g. Lammer et al., 2006; Luhmann and Kozyra, 1991). With the development of new high sensitivity, high angular resolution energetic neutral atom (ENA) instruments, the sputtered oxygen may finally be measured. This is an important contribution to the investigation of the atmospheric evolution, as the sputtering

may provide as much as an additional 30 % to the total escape from the Venusian atmosphere (see Table 3.1). Therefore, future missions should include ENA instruments that can determine the total contribution from sputtering, and how it varies with, for example, upstream parameters.

7.4.4 Ongoing Mission Concepts

Even though there has already been a lot of interest in Venus with measurements made by the 10s of different spacecraft that visited Venus (see chapter 1), there is still a lot more to be learnt, evident from the few suggestions in the sections above. There is currently much interest to go back to Venus again. Mars has been the largest interest for many years now, with currently eight active missions, while Venus has only one active mission: Akatsuki (Nakamura et al., 2011), which unfortunately does not include any dedicated plasma instruments. The interest of sending a new mission to Venus is on the rise, with the inclusion of several space nations in the world. First of all, there are many missions in the coming years that will make flybys of Venus, on their way to other destinations. These missions will provide snapshots of the Venusian plasma environment as they flyby at great speeds. Even so, they will provide new interesting insights into the Venusian plasma environment as we move towards a new solar maximum. The many new upcoming flyby missions are included in Figure 1.1, which also shows the energy range of the ion and electron instruments, and a short description of the missions is included below.

The Parker Solar Probe mission, which was launched in 2018, is designed to make measurements of the Sun and the solar wind (Fox et al., 2016). The pericentre of the orbit will closely approach the Sun and will reach as close as within $\sim 9 R_{\text{SUN}}$ from the solar surface. This mission will have six flybys of Venus, between 2018-2024, and includes several plasma instruments. It has already conducted three of its flybys of Venus, and the data is currently being processed and analysed. The Solar Orbiter, another mission to study the Sun and the solar wind but with a higher inclination (compared to Parker Solar Probe) of the orbit around the Sun, was launched in early 2020. It will make eight Venus flybys between 2020-2030 (Müller et al., 2013). The Parker Solar Probe and Solar Orbiter missions include instruments to measure the SEPs, in addition to ion and electron instruments. If there is any SEP events during one of their flybys, they might be able to measure both the SEP spectra, and the response of the Venusian plasma environment (see subsection 7.4.1). The BepiColombo mission (Benkhoff et al., 2010), currently on its way to Mercury, will make two flybys of Venus during 2020-2021 (see Figure 7.3), where the plasma and ENA instruments will be operational and could thus potentially be the first mission to measure the sputtering from Venus (see subsection 7.4.3). The JUICE mission, aimed to study the Jovian icy moons, will make one flyby of Venus in 2023 on its way to Jupiter (Grasset et al., 2013). The JUICE mission will include an advanced ENA instrument, JNA, which could also potentially measure the sputtering from Venus, if JNA is operational during the Venusian flyby.

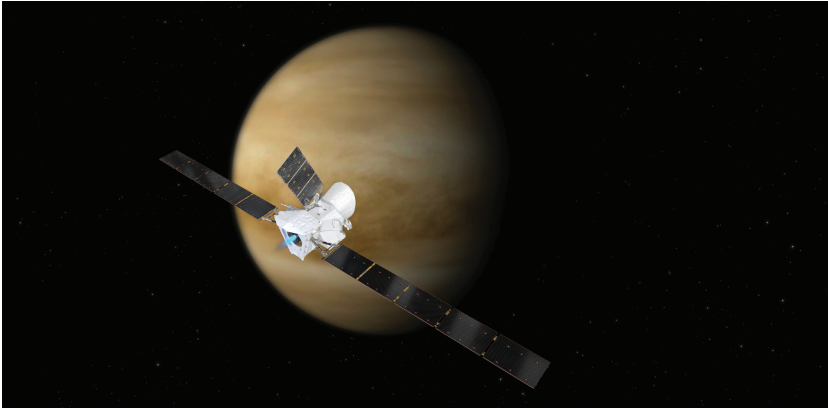


Figure 7.3: An artist’s visualisation of the BepiColombo mission during its flyby of Venus (Benkhoff et al., 2010). Courtesy of ESA.

In addition to the many flybys of Venus in the coming years, there are currently several missions proposed to make dedicated studies at Venus (see detailed summary by Glaze et al., 2018). ISRO, the Indian Space Research Organisation, is planning to send a mission to Venus in 2024. This mission will include a plasma package that will study the Venusian plasma environment further, together with an ENA sensor that the Swedish Institute of Space Physics will provide (private communication with Dr. Y. Futaana). This would be a great addition as it could contribute to the long-term statistics of the plasma environment of Venus. One important part is to get statistics from several more solar cycles with varying activity levels to further study the differences between results from different missions and to understand the variations over the solar cycle. The ENA sensor will attempt to measure the important sputtering from Venus (subsection 7.4.3). In addition, if the orbit insertion of the Indian Venus mission or of any other orbiter mission below, occurs before the last flybys of the above mentioned flyby missions, several multipoint measurements can be made (see discussion in subsection 7.4.1).

The EnVision mission, proposed as an ESA M5 class mission, is aimed to study the geological activity and its relation with the atmosphere. The mission is proposed to have a low circular polar orbit at ~ 260 km (Ghail et al., 2017). This orbit is ideal for completing the previous measurements by PVO and VEx by providing a global map of the ion flows and acceleration processes in the upper ionosphere. For example, it could connect the measurements of the ion flows by PVO near the equator and by VEx near the North Pole (see chapter 5), and connect the low altitude ion acceleration processes with those measured in the Venusian magnetotail and magnetosheath, to answer the “first few eV” question. The mission is currently not designed to include plasma instruments, but it would truly be invaluable if it did include ion and electron instruments

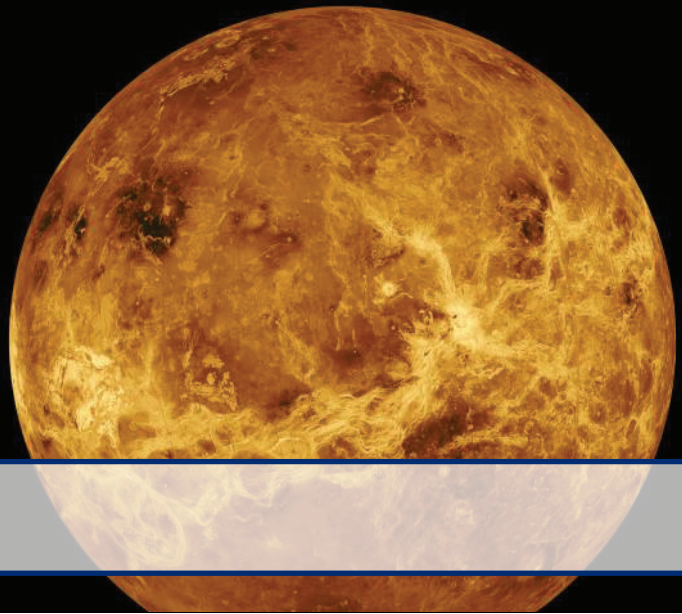
with a high time resolution and a low-to-medium energy range.

There are currently two out of four proposals evaluated in the NASA's discovery class, that is aimed to study Venus: Veritas and DAVINCI+. Veritas will study the surface processes using radar instruments with a higher spatial resolution than previous missions, such as Magellan and VEx (Smrekar et al., 2020). Veritas is designed to make several aerobraking campaigns down to below 130 km. This provides an excellent opportunity to study the ionosphere with further details. The mission design does not currently include plasma instruments, but should also incorporate a high time resolution, medium-to-high mass resolution, low energy ion spectrometer. The most important part would be to measure the low energy ions at a high time resolution in this region. Here, the mission could provide unique measurements of the ion flows and its coupling with the neutral atmosphere (if also including a neutral spectrometer), as described in subsection 7.4.2. DAVINCI+ is a lander, which will impact on Venus and is aimed to survive for a longer time than the latest lander from the Venera missions (Garvin et al., 2020). Using the 21st century instrument technologies, the probe will provide new measurements of the Venusian atmosphere and surface. These measurements can provide more insight into the interaction between the surface and the atmosphere, an important part for the evolution of the Venusian atmosphere. As the results of this thesis point towards only a small contribution to the atmospheric evolution from the escape to space over the past 3.9 Ga (see chapter 6), it is important to understand how the interaction with the surface might have provided the loss of oxygen from the atmosphere. In addition, the mission will measure the D/H ratio with a high resolution as it descends through the atmosphere, which will show variations in the ratio. The D/H ratio and its variations is important as it is the main evidence showing that water was present on Venus in its earlier history. Any variations in the ratio can tell us if the assumption of a historically large water inventory is valid or not.

Russia is also investigating a new mission, Venera-D, as a continuation of the many previous Venera missions. It is a comprehensive mission, which will include an orbiter, a lander, two balloons and several micropubes (Senske et al., 2017). This mission will include plasma instruments to further study the solar wind interaction with Venus, with a higher time resolution. This can provide more details on the acceleration processes at Venus, and the formation of the plasma boundaries. These are important details for a better understanding of the escape from Venus and how this has affected the atmospheric evolution. The baseline orbit is proposed to be similar to the VEx orbit, a 24 hour orbit with a ~ 300 km nominal periapsis. Similar to the Indian Venus mission this can add to the long term statistical variations of the environment, over varying upstream conditions, and provide data from more extreme events. If the mission also includes an instrument to measure the SEPs, with their MeV energies, the potential effect of the SEPs can be further investigated (see subsection 7.4.1). In addition, if the mission makes several aerobraking campaigns, and put the periapsis near the south pole instead of the North Pole, new unique measurements

of the ion flows can be made (see chapter 5).

The suggestion, as described above, is of course that all of these missions include a plasma consortium, if they have not already, as it would provide invaluable additional information needed to further improve the understanding of the Venusian plasma environment and its interaction with the solar wind. However, studying the surface-atmosphere interactions and the D/H ratio are also important for determining the atmospheric evolution of Venus and will aid in the continued task to provide the answer to the key question: Where did the water on Venus go?



Bibliography

- Airapetian, Vladimir S. and Arcadi V. Usmanov (2016). “Reconstructing the Solar Wind from Its Early History to Current Epoch”. In: *The Astrophysical Journal Letters* 817.2, p. L24. URL: <http://stacks.iop.org/2041-8205/817/i=2/a=L24> (cit. on p. 48).
- Albarède, F. (2009). “Volatile accretion history of the terrestrial planets and dynamic implications”. In: *Nature* 461, pp. 1227–1233. URL: <http://dx.doi.org/10.1038/nature08477> (cit. on p. 53).
- Alfvén, H. (1957). “On the Theory of Comet Tails”. In: *Tellus* 9.1, pp. 92–96. DOI: [10.1111/j.2153-3490.1957.tb01855.x](https://doi.org/10.1111/j.2153-3490.1957.tb01855.x) (cit. on p. 10).
- Angsmann, A., M. Fränz, E. Dubinin, et al. (2011). “Magnetic states of the ionosphere of Venus observed by Venus Express”. In: *Planetary and Space Science* 59, pp. 327–337. DOI: [10.1016/j.pss.2010.12.004](https://doi.org/10.1016/j.pss.2010.12.004) (cit. on p. 13).
- Arney, Dale C. and Christopher A. Jones (2015). “High Altitude Venus Operational Concept (HAVOC): An Exploration Strategy for Venus”. In: *AIAA SPACE 2015 Conference and Exposition*. DOI: [10.2514/6.2015-4612](https://doi.org/10.2514/6.2015-4612) (cit. on p. 55).
- Bains, William et al. (2020). *Phosphine on Venus Cannot be Explained by Conventional Processes*. arXiv: 2009.06499 [astro-ph.EP] (cit. on p. 54).
- Barabash, S., A. Fedorov, J. J. Sauvaud, R. Lundin, et al. (2007a). “The loss of ions from Venus through the plasma wakes”. In: *Nature* 450, pp. 650–653. DOI: [10.1038/nature06434](https://doi.org/10.1038/nature06434) (cit. on pp. 15, 20, 21).
- Barabash, S. et al. (2007b). “The analyser of space plasmas and energetic atoms (ASPERA-4) for the Venus Express mission”. In: *Planetary and Space Science*

- Science* 55, pp. 1772–1792. DOI: [10.1016/j.pss.2007.01.014](https://doi.org/10.1016/j.pss.2007.01.014) (cit. on pp. 26, 28).
- Benkhoff, Johannes et al. (2010). “BepiColombo - Comprehensive exploration of Mercury: Mission overview and science goals”. In: *Planetary and Space Science* 58.1, pp. 2–20. DOI: <https://doi.org/10.1016/j.pss.2009.09.020> (cit. on pp. 59, 60).
- Brace, L. H., W. T. Kasprzak, H. A. Taylor, et al. (1987). “The ionotail of Venus: Its configuration and evidence for ion escape”. In: *Journal of Geophysical Research* 92.A1, pp. 15–26 (cit. on pp. 21, 23).
- Brace, L.H., R.F. Theis, and W.R. Hoegy (1982). “Plasma clouds above the ionopause of Venus and their implications”. In: *Planetary and Space Science* 30.1, pp. 29–37. DOI: [https://doi.org/10.1016/0032-0633\(82\)90069-1](https://doi.org/10.1016/0032-0633(82)90069-1) (cit. on p. 21).
- Breus, T. K. (1979). “Venus: Review of present understanding of solar wind interaction”. In: *Space Science Reviews* 23, pp. 253–275 (cit. on p. 2).
- Bridge, H. S., A. J. Lazarus, G. L. Siscoe, et al. (1976). “Interaction of the solar wind with Venus”. In: *Solar wind interaction with the planets Mercury, Venus, and Mars*. Ed. by N. F. Ness. Vol. SP-397. USSR. Moscow, USSR: NASA, pp. 63–79 (cit. on p. 2).
- Butler, D. M. and J. W. Chamberlain (1976). “Venus’ night side ionosphere: Its origin and maintenance”. In: *Journal of Geophysical Research* 81.25, pp. 4757–4760. ISSN: 2156-2202. DOI: [10.1029/JA081i025p04757](https://doi.org/10.1029/JA081i025p04757) (cit. on p. 8).
- Carlsson, E. et al. (2006). “Mass composition of the escaping plasma at Mars”. In: *Icarus* 182.2, pp. 320–328. DOI: [10.1016/j.icarus.2005.09.020](https://doi.org/10.1016/j.icarus.2005.09.020) (cit. on p. 30).
- Catling, David C. and James F. Kasting (2017). “Escape of Atmospheres to Space”. In: *Atmospheric Evolution on Inhabited and Lifeless Worlds*. Cambridge University Press, pp. 129–168. DOI: [10.1017/9781139020558.006](https://doi.org/10.1017/9781139020558.006) (cit. on p. 16).
- Chamberlain, Joseph W. (1963). “Planetary coronae and atmospheric evaporation”. In: *Planetary and Space Science* 11.8, pp. 901–960. DOI: [10.1016/0032-0633\(63\)90122-3](https://doi.org/10.1016/0032-0633(63)90122-3) (cit. on p. 16).
- Chassefière, E. (1996). “Hydrodynamic Escape of Oxygen from Primitive Atmospheres: Applications to the Cases of Venus and Mars”. In: *Icarus* 124.2, pp. 537–552. DOI: [10.1006/icar.1996.0229](https://doi.org/10.1006/icar.1996.0229) (cit. on p. 17).
- Colin, L. (1980). “The Pioneer Venus Program”. In: *Journal of Geophysical Research: Space Physics* 85.A13, pp. 7575–7598. DOI: [10.1029/JA085iA13p07575](https://doi.org/10.1029/JA085iA13p07575) (cit. on p. 2).

- Collinson, G. A., R. A. Frahm, A. Gloer, A. J. Coates, et al. (2016). "The electric wind of Venus: A global and persistent "polar wind"-like ambipolar electric field sufficient for the direct escape of heavy ionospheric ions". In: *Geophysical Research Letters* 43. DOI: 10.1002/2016GL068327 (cit. on p. 20).
- Dimmock, A. P. et al. (2018). "The Response of the Venusian Plasma Environment to the Passage of an ICME: Hybrid Simulation Results and Venus Express Observations". In: *Journal of Geophysical Research: Space Physics* 123.5, pp. 3580–3601. DOI: 10.1029/2017JA024852 (cit. on pp. 56, 57).
- Donahue, T. M., D. H. Grinspoon, R. E. Hartle, and R. R. Hodges Jr. (1997). "Ion/neutral Escape of Hydrogen and Deuterium: Evolution of Water". In: *Venus II: Geology, Geophysics, Atmosphere, and Solar Wind Environment*. Ed. by S. W. Bougher, D. M. Hunten, and R. J. Phillips, p. 385 (cit. on pp. 3, 53).
- Donahue, Thomas M. and Richard E. Hartle (1992). "Solar cycle variations in H⁺ and D⁺ densities in the Venus ionosphere: Implications for escape". In: *Geophysical Research Letters* 19.24, pp. 2449–2452. DOI: 10.1029/92GL02927 (cit. on pp. 3, 18, 53).
- Dubinin, E. et al. (2011). "Ion Energization and Escape on Mars and Venus". In: *Space Science Reviews* 162.1, pp. 173–211. DOI: 10.1007/s11214-011-9831-7 (cit. on pp. 10, 17, 20).
- Edberg, N. J. T. et al. (2011). "Atmospheric erosion of Venus during stormy space weather". In: *Journal of Geophysical Research: Space Physics* 116.A9. A09308. DOI: 10.1029/2011JA016749 (cit. on pp. 11, 56).
- Efron, B. and R.J. Tibshirani (1994). *An Introduction to the Bootstrap*. Chapman & Hall/CRC Monographs on Statistics & Applied Probability. Taylor & Francis (cit. on p. 36).
- Elphic, R. C., C. T. Russell, J. G. Luhmann, F. L. Scarf, and L. H. Brace (1981). "The Venus ionopause current sheet: Thickness length scale and controlling factors". In: *Journal of Geophysical Research: Space Physics* 86.A13, pp. 11430–11438. DOI: 10.1029/JA086iA13p11430 (cit. on p. 13).
- Erkaev, Nikolai V. et al. (2013). "XUV-Exposed, Non-Hydrostatic Hydrogen-Rich Upper Atmospheres of Terrestrial Planets. Part I: Atmospheric Expansion and Thermal Escape". In: *Astrobiology* 13.11, pp. 1011–1029. DOI: 10.1089/ast.2012.0957 (cit. on p. 16).
- Fedorov, A., S. Barabash, J. A. Sauvaud, et al. (2011). "Measurements of the ion escape rates from Venus for solar minimum". In: *Journal of Geophysical Research* 116, A07220. DOI: 10.1029/2011JA016427 (cit. on pp. 14, 21, 23, 24, 31, 32, 43).

- Fox, J. L. and K. Y. Sung (2001). “Solar activity variations of the Venus thermosphere/ionosphere”. In: *Journal of Geophysical Research* 106.A10, pp. 21305–21335. DOI: 10.1029/2001JA000069 (cit. on pp. 8, 9, 30, 31, 40, 41).
- Fox, Jane L. and Aleksander B. Hać (2009). “Photochemical escape of oxygen from Mars: A comparison of the exobase approximation to a Monte Carlo method”. In: *Icarus* 204.2, pp. 527–544. DOI: 10.1016/j.icarus.2009.07.005 (cit. on p. 18).
- Fox, N. J. et al. (2016). “The Solar Probe Plus Mission: Humanity’s First Visit to Our Star”. In: *Space Science Reviews* 204.1, pp. 7–48. DOI: 10.1007/s11214-015-0211-6 (cit. on p. 59).
- Futaana, Y., G. Stenberg Wieser, S. Barabash, and J. G. Luhmann (2017). “Solar Wind Interaction and Impact on the Venus Atmosphere”. In: *Space Science Reviews* 212.3, pp. 1453–1509. DOI: 10.1007/s11214-017-0362-8 (cit. on pp. 3, 5, 11, 17, 21, 23, 41).
- Futaana, Y., S. Barabash, M. Yamauchi, S. McKenna-Lawlor, R. Lundin, J.G. Luhmann, et al. (2008). “Mars Express and Venus Express multi-point observations of geoeffective solar flare events in December 2006”. In: *Planetary and Space Science* 56.6. Mars Express/Venus Express, pp. 873–880. DOI: 10.1016/j.pss.2007.10.014 (cit. on pp. 11, 57).
- Garvin, J. B. et al. (2020). “DAVINCI+: Deep Atmosphere of Venus Investigation of Noble Gases, Chemistry, and Imaging Plus”. In: *51st Lunar and Planetary Science Conference, held 16-20 March, 2020 at The Woodlands, Texas. LPI Contribution No. 2326, 2020, id.2599* (cit. on p. 61).
- Ghail, R., C. Wilson, T. Widemann, L. Bruzzone, C. Dumoulin, J. Helbert, et al. (2017). “EnVision: Understanding why our most Earth-like neighbour is so different”. In: *arXiv e-prints*. DOI: arXiv:1703.09010 (cit. on p. 60).
- Gillmann, C and P. Tackley (2014). “Atmosphere/mantle coupling and feedbacks on Venus”. In: *Journal of Geophysical Research: Planets* 119.6, pp. 1189–1217. DOI: 10.1002/2013JE004505 (cit. on pp. 17, 53).
- Glaze, Lori S., Colin F. Wilson, Liudmila V. Zasova, Masato Nakamura, and Sanjay Limaye (2018). “Future of Venus Research and Exploration”. In: *Space Science Reviews* 214.5, p. 89. DOI: 10.1007/s11214-018-0528-z (cit. on p. 60).
- Grasset, O. et al. (2013). “JUperiter ICy moons Explorer (JUICE): An ESA mission to orbit Ganymede and to characterise the Jupiter system”. In: *Planetary and Space Science* 78, pp. 1–21. DOI: 10.1016/j.pss.2012.12.002 (cit. on p. 59).

- Greaves, Jane S. et al. (2020). “Phosphine gas in the cloud decks of Venus”. In: *Nature Astronomy*. DOI: [10.1038/s41550-020-1174-4](https://doi.org/10.1038/s41550-020-1174-4) (cit. on p. 54).
- Gringauz, K. I., V. V. Bezrukikh, L. S. Musatov, and T. K. Breus (1968). “Plasma measurements in the vicinity of Venus by the space vehicle Venus-4”. In: *Cosmic Research (USSR)* 6.350 (cit. on p. 2).
- Grinspoon, D. H. (1993). “Implications of the high D/H ratio for the sources of water in Venus’ atmosphere”. In: *Nature* 363, pp. 428–431. DOI: [10.1038/363428a0](https://doi.org/10.1038/363428a0) (cit. on pp. 3, 53).
- Grisson, Benjamin et al. (2018). “Shock deceleration in interplanetary coronal mass ejections (ICMEs) beyond Mercury’s orbit until one AU”. In: *J. Space Weather Space Clim.* 8, A54. DOI: [10.1051/swsc/2018043](https://doi.org/10.1051/swsc/2018043) (cit. on p. 11).
- Harada, Y. et al. (2015). “Magnetic reconnection in the near-Mars magnetotail: MAVEN observations”. In: *Geophysical Research Letters* 42.21, pp. 8838–8845. DOI: [10.1002/2015GL065004](https://doi.org/10.1002/2015GL065004) (cit. on p. 46).
- Harada, Y. et al. (2017). “Survey of magnetic reconnection signatures in the Martian magnetotail with MAVEN”. In: *Journal of Geophysical Research: Space Physics* 122.5, pp. 5114–5131. DOI: [10.1002/2017JA023952](https://doi.org/10.1002/2017JA023952) (cit. on p. 46).
- Hedin, A. E., H. B. Niemann, W. T. Kasprzak, and A. Seiff (1983). “Global empirical model of the Venus thermosphere”. In: *Journal of Geophysical Research* 88.A1, pp. 73–83. DOI: [10.1029/JA088iA01p00073](https://doi.org/10.1029/JA088iA01p00073) (cit. on pp. 8, 9).
- Horinouchi, Takeshi et al. (2020). “How waves and turbulence maintain the super-rotation of Venus’ atmosphere”. In: *Science* 368.6489, pp. 405–409. DOI: [10.1126/science.aaz4439](https://doi.org/10.1126/science.aaz4439) (cit. on p. 7).
- Jarvinen, R., E. Kallio, and S. Dyadechkin (2013). “Hemispheric asymmetries of the Venus plasma environment”. In: *Journal of Geophysical Research* 118, pp. 4551–4563. DOI: [10.1002/jgra.50387](https://doi.org/10.1002/jgra.50387) (cit. on pp. 14, 31, 35).
- Jeans, J. H. (1925). *The dynamical theory of gases*. Cambridge University Press, p. 444 (cit. on p. 16).
- Johnstone, C. P., M. Güdel, H. Lammer, and K. G. Kislyakova (2018). “Upper atmospheres of terrestrial planets: Carbon dioxide cooling and the Earth’s thermospheric evolution”. In: *A&A* 617, A107. DOI: [10.1051/0004-6361/201832776](https://doi.org/10.1051/0004-6361/201832776) (cit. on p. 16).
- Kasting, James F. and James B. Pollack (1983). “Loss of water from Venus. I. Hydrodynamic escape of hydrogen”. In: *Icarus* 53.3, pp. 479–508. DOI: [10.1016/0019-1035\(83\)90212-9](https://doi.org/10.1016/0019-1035(83)90212-9) (cit. on pp. 16, 17, 53).

- Keating, G. M., J. L. Bertaux, S. W. Bougher, et al. (1985). “Models of Venus neutral upper atmosphere: structure and composition”. In: *Advances in Space Research* 5.11, pp. 117–171 (cit. on p. 8).
- Knudsen, W. C., K. Spenner, and K. L. Miller (1981). “Anti-solar acceleration of ionospheric plasma across the Venus terminator”. In: *Geophysical Research Letters* 8.3, pp. 241–244. DOI: [10.1029/GL008i003p00241](https://doi.org/10.1029/GL008i003p00241) (cit. on p. 9).
- Knudsen, W. C., K. Spenner, K. L. Miller, and V. Novak (1980). “Transport of ionospheric O⁺ ions across the Venus terminator and implications”. In: *Journal of Geophysical Research* 85.A13, pp. 7803–7810. DOI: [10.1029/JA085iA13p07803](https://doi.org/10.1029/JA085iA13p07803) (cit. on pp. 8, 28, 39).
- Knudsen, William C. and Kent L. Miller (1992). “The Venus transterminator ion flux at solar maximum”. In: *Journal of Geophysical Research: Space Physics* 97.A11, pp. 17165–17167. DOI: [10.1029/92JA01460](https://doi.org/10.1029/92JA01460) (cit. on pp. 10, 39, 41).
- Kollmann, P., P.C. Brandt, G. A. Collinson, et al. (2016). “Properties of planetward ion flows in Venus’ magnetotail”. In: *Icarus* 274, pp. 73–82. DOI: [10.1016/j.icarus.2016.02.053](https://doi.org/10.1016/j.icarus.2016.02.053) (cit. on pp. 20, 45, 46).
- Lammer, H. (2013). *Origin and evolution of planetary atmospheres: implications for habitability*. Springer Briefs in Astronomy, Springer, Berlin (cit. on pp. 17, 19).
- Lammer, H. et al. (2006). “Loss of hydrogen and oxygen from the upper atmosphere of Venus”. In: *Planetary and Space Science* 54.13. The Planet Venus and the Venus Express Mission, pp. 1445–1456. DOI: [10.1016/j.pss.2006.04.022](https://doi.org/10.1016/j.pss.2006.04.022) (cit. on pp. 16–19, 21, 23, 24, 58).
- Lécuyer, C., L. Simon, and F. Guyot (2000). “Comparison of carbon, nitrogen and water budgets on Venus and the Earth”. In: *Earth and Planetary Science Letters* 181.1, pp. 33–40. DOI: [10.1016/S0012-821X\(00\)00195-3](https://doi.org/10.1016/S0012-821X(00)00195-3) (cit. on p. 53).
- Limaye, Sanjay S., Rakesh Mogul, David J. Smith, Arif H. Ansari, Grzegorz P. Słowik, and Parag Vaishampayan (2018). “Venus’ Spectral Signatures and the Potential for Life in the Clouds”. In: *Astrobiology* 18.9, pp. 1181–1198. DOI: [10.1089/ast.2017.1783](https://doi.org/10.1089/ast.2017.1783) (cit. on p. 54).
- Lindsay, G. M., J. G. Luhmann, C. T. Russell, and J. T. Gosling (1999). “Relationships between coronal mass ejection speeds from coronagraph images and interplanetary characteristics of associated interplanetary coronal mass ejections”. In: *Journal of Geophysical Research: Space Physics* 104.A6, pp. 12515–12523. DOI: [10.1029/1999JA900051](https://doi.org/10.1029/1999JA900051) (cit. on p. 11).

- Luhmann, J. G. and S. J. Bauer (1992). "Solar Wind Effects on Atmosphere Evolution at Venus and Mars". In: pp. 417–430. DOI: *10.1029/GM066p0417* (cit. on pp. 19, 23).
- Luhmann, J. G. and T. E. Cravens (1991). "Magnetic fields in the ionosphere of Venus". In: *Space Science Reviews* 55, pp. 201–274. DOI: *10.1007/BF00177138* (cit. on p. 13).
- Luhmann, J. G. and J. U. Kozyra (1991). "Dayside pickup oxygen ion precipitation at Venus and Mars: Spatial distributions, energy deposition and consequences". In: *Journal of Geophysical Research* 96.A4, pp. 5457–5467. DOI: *10.1029/90JA01753* (cit. on pp. 19, 23, 58).
- Luhmann, J. G., S. A. Ledvina, J. G. Lyon, and C. T. Russell (2006). "Venus O⁺ pickup ions: Collected PVO results and expectations for Venus Express". In: *Planetary and Space Science* 54, pp. 1457–1471 (cit. on pp. 11, 19, 56).
- Luhmann, Janet G. (1986). "The solar wind interaction with Venus". In: *Space Science Reviews* 44, pp. 241–306 (cit. on pp. 11, 12).
- Luhmann, J.G. et al. (2015). "Solar wind interaction effects on the magnetic fields around Mars: Consequences for interplanetary and crustal field measurements". In: *Planetary and Space Science* 117, pp. 15–23. DOI: *10.1016/j.pss.2015.05.004* (cit. on p. 46).
- Lundin, R., H. Lammer, and I. Ribas (2007). "Planetary magnetic fields and solar forcing: implications for atmospheric evolution". In: *Space Science Reviews* 129, pp. 245–278. DOI: *10.1007/s11214-007-9176-4* (cit. on p. 20).
- Lundin, R., S. Barabash, Y. Futaana, et al. (2011). "Ion flow and momentum transfer in the Venus plasma environment". In: *Icarus* 215, pp. 751–758. DOI: *10.1016/j.icarus.2011.06.034* (cit. on pp. 40–42).
- Lundin, R., S. Barabash, Y. Futaana, et al. (2014). "Solar wind-driven thermospheric winds over the Venus North Polar region". In: *Geophysical Research Letters* 41, pp. 4413–4419. DOI: *10.1002/2014GL060605* (cit. on pp. 9, 40, 41).
- Marov, M. Y. (1972). "Venus: A perspective at the beginning of planetary exploration". In: *Icarus* 16, pp. 415–461 (cit. on p. 2).
- Martinecz, C., M. Fränz, J. Woch, et al. (2008). "Location of the bow shock and ion composition boundary at Venus - initial determinations from Venus Express ASPERA-4". In: *Planetary and Space Science* 56, pp. 780–784. DOI: *10.1016/j.pss.2007.07.007* (cit. on p. 45).
- Masunaga, K. et al. (2019). "Effects of the solar wind and the solar EUV flux on O⁺ escape rates from Venus". In: *Icarus* 321, pp. 379–387. DOI: *10.1016/j.icarus.2018.11.017* (cit. on pp. 19, 23, 45, 48).

- Mayyasi, Majd, C. Narvaez, Mehdi Benna, M. Elrod, and Paul Mahaffy (2019). “Ion-Neutral Coupling in the Upper Atmosphere of Mars: A Dominant Driver of Topside Ionospheric Structure”. In: *Journal of Geophysical Research: Space Physics* ja. DOI: 10.1029/2019JA026481 (cit. on p. 58).
- McComas, D. J., H. E. Spence, C. T. Russell, and M. A. Saunders (1986). “The average magnetic field draping and consistent plasma properties of the Venus magnetotail”. In: *Journal of Geophysical Research: Space Physics* 91.A7, pp. 7939–7953. DOI: 10.1029/JA091iA07p07939 (cit. on pp. 21, 23, 35).
- McEnulty, T.R. et al. (2010). “Interplanetary coronal mass ejection influence on high energy pick-up ions at Venus”. In: *Planetary and Space Science* 58.14, pp. 1784–1791. DOI: 10.1016/j.pss.2010.07.019 (cit. on pp. 19, 56).
- Merino, Nancy et al. (2019). “Living at the Extremes: Extremophiles and the Limits of Life in a Planetary Context”. In: *Frontiers in Microbiology* 10, p. 780. DOI: 10.3389/fmicb.2019.00780 (cit. on p. 54).
- Miller, K. L. and R. C. Whitten (1991). “Ion dynamics in the Venus ionosphere”. In: *Space Science Reviews* 55, pp. 165–199. DOI: 10.1007/BF00177137 (cit. on pp. 39, 40).
- Morowitz, H. and C. Sagan (1967). “Life in the Clouds of Venus?” In: *Nature* 215.5107, pp. 1259–1260. DOI: 10.1038/2151259a0 (cit. on p. 2).
- Müller, D., R. G. Marsden, O. C. St. Cyr, H. R. Gilbert, and The Solar Orbiter Team (2013). “Solar Orbiter”. In: *Solar Physics* 285.1, pp. 25–70. DOI: 10.1007/s11207-012-0085-7 (cit. on p. 59).
- Müller-Wodarg, Ingo C. F., Sean Bruinsma, Jean-Charles Marty, and Håkan Svedhem (2016). “In situ observations of waves in Venus’s polar lower thermosphere with Venus Express aerobraking Venus’s polar lower thermosphere with Venus Express aerobraking”. In: *Nature Physics*. DOI: 10.1038/NPHYS3733 (cit. on p. 58).
- Nakamura, M. et al. (2011). “Overview of Venus orbiter, Akatsuki”. In: *Earth, Planets and Space* 63.5, pp. 443–457. DOI: 10.5047/eps.2011.02.009 (cit. on p. 59).
- Niemann, H. B., J. R. Booth, J. E. Cooley, et al. (1980). “Pioneer Venus Orbiter Neutral Gas Mass Spectrometer Experiment”. In: *IEEE Transactions on Geoscience and Remote Sensing* GE-18.1, pp. 60–65 (cit. on p. 8).
- Nilsson, H. et al. (2012). “Ion distributions in the vicinity of Mars: Signatures of heating and acceleration processes”. In: *Earth, Planets and Space* 64.2, p. 9. DOI: 10.5047/eps.2011.04.011 (cit. on pp. 20, 32).
- Nordheim, T.A., L.R. Dartnell, L. Desorgher, A.J. Coates, and G.H. Jones (2015). “Ionization of the venusian atmosphere from solar and galactic

- cosmic rays”. In: *Icarus* 245, pp. 80–86. DOI: <https://doi.org/10.1016/j.icarus.2014.09.032> (cit. on p. 55).
- Nordström, T., G. Stenberg, H. Nilsson, S. Barabash, and T. L. Zhang (2013). “Venus ion outflow estimates at solar minimum: Influence of reference frames and disturbed solar wind conditions”. In: *Journal of Geophysical Research: Space Physics* 118.6, pp. 3592–3601. DOI: [10.1002/jgra.50305](https://doi.org/10.1002/jgra.50305) (cit. on p. 35).
- Parker, E. N. (1958). “Dynamics of the Interplanetary Gas and Magnetic Fields”. In: *The Astrophysical Journal* 128, p. 664 (cit. on p. 10).
- Perez-de-Tejada, H. (1986). “Fluid dynamic constraints of the Venus ionospheric flow”. In: *Journal of Geophysical Research* 91.A6, pp. 6765–6770 (cit. on p. 9).
- Pérez-de-Tejada, H. et al. (2011). “Plasma transition at the flanks of the Venus ionosheath: Evidence from the Venus Express data”. In: *Journal of Geophysical Research: Space Physics* 116.A1. DOI: [10.1029/2009JA015216](https://doi.org/10.1029/2009JA015216) (cit. on p. 20).
- Persson, M. (2015). “Venus Thermosphere Densities as Revealed by Venus Express Torque and Accelerometer Data”. MA thesis. Luleå University of Technology (cit. on p. 58).
- Persson, M., Y. Futaana, A. Fedorov, and S. Barabash (2020c). “Return flows in the Venusian magnetotail measured by Venus Express”. In: *To be submitted for publication in Journal of Geophysical Research: Space Physics* (cit. on pp. 45, 46).
- Persson, M., Y. Futaana, A. Fedorov, H. Nilsson, M. Hamrin, and S. Barabash (2018). “H⁺/O⁺ Escape Rate Ratio in the Venus Magnetotail and its Dependence on the Solar Cycle”. In: *Geophysical Research Letters* 45.20, pp. 10, 805–10, 811. DOI: [10.1029/2018GL079454](https://doi.org/10.1029/2018GL079454) (cit. on pp. 32, 36, 44, 45, 52).
- Persson, M. et al. (2019). “Heavy ion flows in the upper ionosphere of the Venusian North Pole”. In: *Journal of Geophysical Research: Space Physics*. DOI: [10.1029/2018JA026271](https://doi.org/10.1029/2018JA026271) (cit. on pp. 28, 29, 31, 39–41).
- Persson, M. et al. (2020a). “The Venusian Atmospheric Oxygen Ion Escape: Extrapolation to the Early Solar System”. In: *Journal of Geophysical Research: Planets* 125.3. DOI: [10.1029/2019JE006336](https://doi.org/10.1029/2019JE006336) (cit. on pp. 47, 49, 52, 56).
- Persson, M. et al. (2020b). “Global Venus-Solar Wind Coupling and Oxygen Ion Escape”. In: *Submitted for publication in Geophysical Research Letters* (cit. on pp. 47, 48, 52).
- Pierrard, V (2003). “Evaporation of hydrogen and helium atoms from the atmospheres of Earth and Mars”. In: *Planetary and Space Science* 51.4, pp. 319–327. DOI: [10.1016/S0032-0633\(03\)00014-X](https://doi.org/10.1016/S0032-0633(03)00014-X) (cit. on p. 16).

- Ramstad, R., S. Barabash, Y. Futaana, H. Nilsson, X.-D. Wang, and M. Holmström (2015). “The Martian atmospheric ion escape rate dependence on solar wind and solar EUV conditions: 1. Seven years of Mars Express observations”. In: *Journal of Geophysical Research: Planets* 120, pp. 1298–1309. DOI: [10.1002/2015JE004816](https://doi.org/10.1002/2015JE004816) (cit. on p. 52).
- Ramstad, Robin, Stas Barabash, Yoshifumi Futaana, Hans Nilsson, and Mats Holmström (2017). “Global Mars-solar wind coupling and ion escape”. In: *Journal of Geophysical Research: Space Physics*. DOI: [10.1002/2017JA024306](https://doi.org/10.1002/2017JA024306) (cit. on pp. 41, 52).
- Ramstad, Robin, Stas Barabash, Yoshifumi Futaana, Hans Nilsson, and Mats Holmström (2018). “Ion Escape From Mars Through Time: An Extrapolation of Atmospheric Loss Based on 10 Years of Mars Express Measurements”. In: *Journal of Geophysical Research: Planets* 123.11, pp. 3051–3060. DOI: [10.1029/2018JE005727](https://doi.org/10.1029/2018JE005727) (cit. on p. 52).
- Read, Peter L. and Sebastien Lebonnois (2018). “Superrotation on Venus, on Titan, and Elsewhere”. In: *Annual Review of Earth and Planetary Sciences* 46.1, pp. 175–202. DOI: [10.1146/annurev-earth-082517-010137](https://doi.org/10.1146/annurev-earth-082517-010137) (cit. on p. 7).
- Reames, Donald V. (1999). “Particle acceleration at the Sun and in the heliosphere”. In: *Space Science Reviews* 90.3, pp. 413–491. DOI: [10.1023/A:1005105831781](https://doi.org/10.1023/A:1005105831781) (cit. on p. 56).
- Richardson, Ian G. (2018). “Solar wind stream interaction regions throughout the heliosphere”. In: *Living Reviews in Solar Physics* 15.1, p. 1. DOI: [10.1007/s41116-017-0011-z](https://doi.org/10.1007/s41116-017-0011-z) (cit. on p. 11).
- Rong, Z. J. et al. (2014). “Morphology of magnetic field in near-Venus magnetotail: Venus express observations”. In: *Journal of Geophysical Research: Space Physics* 119.11, pp. 8838–8847. DOI: [10.1002/2014JA020461](https://doi.org/10.1002/2014JA020461) (cit. on p. 45).
- Rothschild, Lynn (2007). “Extremophiles: defining the envelope for the search for life in the universe”. In: *Planetary Systems and the Origins of Life*. Ed. by R. Pudritz, P. Higgs, and J. Stone. Cambridge University Press, p. 113 (cit. on p. 54).
- Russell, C. T. (1991). “Venus Aeronomy”. In: *Space Science Reviews* 55.1-4. DOI: [10.1007/978-94-011-3300-5](https://doi.org/10.1007/978-94-011-3300-5) (cit. on p. 11).
- Russell, C. T. and R. C. Elphic (1979). “Observations of magnetic flux ropes in the Venus ionosphere”. In: *Nature* 279.5714, pp. 616–618 (cit. on p. 13).
- Russell, C. T., J. G. Luhmann, R. C. Elphic, F. L. Scarf, and L. H. Brace (1982). “Magnetic field and plasma wave observations in a plasma cloud

- at Venus". In: *Geophysical Research Letters* 9.1, pp. 45–48. DOI: 10.1029/GL009i001p00045 (cit. on p. 21).
- Saunders, M. A. and C. T. Russell (1986). "Average dimension and magnetic structure of the distant Venus magnetotail". In: *Journal of Geophysical Research: Space Physics* 91.A5, pp. 5589–5604. DOI: 10.1029/JA091iA05p05589 (cit. on p. 12).
- Savani, N. P. et al. (2011). "Evolution of coronal mass ejection morphology with increasing heliocentric distance. II. In situ observations." In: *The Astrophysical Journal* 732.2, p. 117. DOI: 10.1088/0004-637x/732/2/117 (cit. on p. 11).
- Schillings, Audrey, Rikard Slapak, Hans Nilsson, Masatoshi Yamauchi, Iannis Dandouras, and Lars-Göran Westerberg (2019). "Earth atmospheric loss through the plasma mantle and its dependence on solar wind parameters". In: *Earth, Planets and Space* 71.1, p. 70. DOI: 10.1186/s40623-019-1048-0 (cit. on p. 52).
- Schubert, G., C. Covey, A. Del Genio, et al. (1980). "Structure and circulation of the Venus atmosphere". In: *Journal of Geophysical Research* 85.A13, pp. 8007–8025 (cit. on p. 7).
- Schulze-Makuch, Dirk, David H. Grinspoon, Ousama Abbas, Louis N. Irwin, and Mark A. Bullock (2004). "A Sulfur-Based Survival Strategy for Putative Phototrophic Life in the Venusian Atmosphere". In: *Astrobiology* 4.1, pp. 11–18. DOI: 10.1089/153110704773600203 (cit. on p. 54).
- Seager, Sara et al. (2020). "The Venusian Lower Atmosphere Haze as a Depot for Desiccated Microbial Life: A Proposed Life Cycle for Persistence of the Venusian Aerial Biosphere". In: *Astrobiology*. DOI: 10.1089/ast.2020.2244 (cit. on p. 54).
- Senske, D. et al. (2017). "Venera-D: expanding our horizon of terrestrial planet climate and geology through the comprehensive exploration of Venus". In: *Report of the Venera-D Joint Science Definition Team*. URL: <http://www.lpi.usra.edu/vexag/meetings/meetings-of-interest/Venera-D-Report.pdf> (cit. on p. 61).
- Smrekar, S. E. et al. (2020). "Veritas (Venus Emissivity, Radio Science, Insar, Topography, and Spectroscopy): A Proposed Discovery Mission". In: *51st Lunar and Planetary Science Conference, held 16-20 March, 2020 at The Woodlands, Texas. LPI Contribution No. 2326, 2020, id.1449* (cit. on p. 61).
- Svedhem, H. et al. (2007). "Venus Express - The first European mission to Venus". In: *Planetary and Space Science* 55, pp. 1636–1652. DOI: 10.1016/j.pss.2007.01.013 (cit. on pp. 2, 25).

- Taylor, F. and D. Grinspoon (2009). "Climate evolution of Venus". In: *Journal of Geophysical Research: Planets* 114.E9. DOI: 10.1029/2008JE003316 (cit. on pp. 3, 53).
- Taylor, H. A., H. C. Brinton, S. J. Bauer, R. E. Hartle, P. A. Cloutier, and R. E. Daniell (1980). "Global observations of the composition and dynamics of the ionosphere of Venus: Implications for the solar wind interaction". In: *Journal of Geophysical Research: Space Physics* 85.A13, pp. 7765–7777. DOI: 10.1029/JA085iA13p07765 (cit. on pp. 8, 9, 30, 31, 40).
- Tian, Feng (2009). "Thermal Escape from Super Earth Atmospheres in the Habitable Zones of M Stars". In: *The Astrophysical Journal* 703.1, p. 905. URL: <http://stacks.iop.org/0004-637X/703/i=1/a=905> (cit. on p. 17).
- Tu, Lin, Colin P. Johnstone, Manuel Güdel, and Helmut Lammer (2015). "The extreme ultraviolet and X-ray Sun in Time: High-energy evolutionary tracks of a solar-like star". In: *A&A* 577, p. L3. DOI: 10.1051/0004-6361/201526146 (cit. on p. 17).
- Vaisberg, O. et al. (1995). "Ion populations in the tail of Venus". In: *Advances in Space Research* 16.4. Comparative Studies of Magnetospheric Phenomena, pp. 105–118. DOI: [https://doi.org/10.1016/0273-1177\(95\)00217-3](https://doi.org/10.1016/0273-1177(95)00217-3) (cit. on p. 15).
- Vinogradov, A. P., U. A. Surkov, and C. P. Florensky (1968). "The Chemical Composition of the Venus Atmosphere Based on the Data of the Interplanetary Station Venera 4". In: *Journal of the Atmospheric Sciences* 25.4, pp. 535–536. DOI: 10.1175/1520-0469(1968)025<0535:TCCOTV>2.0.CO;2 (cit. on p. 2).
- Wang, C., D. Du, and J. D. Richardson (2005). "Characteristics of the interplanetary coronal mass ejections in the heliosphere between 0.3 and 5.4 AU". In: *Journal of Geophysical Research: Space Physics* 110.A10. DOI: 10.1029/2005JA011198 (cit. on p. 11).
- Way, M. J. and Anthony D. Del Genio (2020). "Venusian Habitable Climate Scenarios: Modeling Venus Through Time and Applications to Slowly Rotating Venus-Like Exoplanets". In: *Journal of Geophysical Research: Planets* 125.5. DOI: 10.1029/2019JE006276 (cit. on p. 53).
- Way, M. J. et al. (2016). "Was Venus the first habitable world of our solar system?" In: *Geophysical Research Letters* 43.16, pp. 8376–8383. DOI: 10.1002/2016GL069790 (cit. on pp. 3, 48).
- Wood, Brian E. (2006). "The Solar Wind and the Sun in the Past". In: *Space Science Reviews* 126.1, pp. 3–14. DOI: 10.1007/s11214-006-9006-0 (cit. on p. 48).

- Wordsworth, R. D. and R. T. Pierrehumbert (2013). “Water Loss from Terrestrial Planets with CO₂-rich Atmospheres”. In: *The Astrophysical Journal* 778.2, p. 154. URL: <http://stacks.iop.org/0004-637X/778/i=2/a=154> (cit. on p. 17).
- Xu, Qi et al. (2019). “Observations of the Venus Dramatic Response to an Extremely Strong Interplanetary Coronal Mass Ejection”. In: *The Astrophysical Journal* 876.1, p. 84. DOI: [10.3847/1538-4357/ab14e1](https://doi.org/10.3847/1538-4357/ab14e1) (cit. on p. 57).
- Zhang, T. L., G. Berghofer, W. Magnes, M. Delva, W. Baumjohann, H. Biernat, et al. (2007). “MAG: The fluxgate magnetometer of Venus Express”. In: *ESA Special Publication SP 1295*, pp. 1–10 (cit. on p. 26).
- Zhang, T. L. et al. (2010). “Hemispheric asymmetry of the magnetic field wrapping pattern in the Venusian magnetotail”. In: *Geophysical Research Letters* 37.14. L14202. DOI: [10.1029/2010GL044020](https://doi.org/10.1029/2010GL044020) (cit. on pp. 35, 45).
- Zhang, T. L. et al. (2012). “Magnetic Reconnection in the Near Venusian Magnetotail”. In: *Science* 336.6081, pp. 567–570. DOI: [10.1126/science.1217013](https://doi.org/10.1126/science.1217013) (cit. on pp. 20, 46).